A study for the roles of Nup133, Nup153 and membrane fenestrae in post-mitotic nuclear pore complex formation

有糸分裂後核膜孔形成における Nup133、Nup153、および開窓膜構造の役割の研究

Ph.D. Thesis

ŞÜKRİYE BİLİR

Osaka University

Graduate School of Frontier Biosciences

2018 January 07

Summary

Nuclear pore complexes (NPC) are gates residing in the nuclear envelope (NE) and responsible for nucleo-cytoplasmic exchange. They are huge protein complexes including 8-fold of ~30 proteins which are called as nucleoporins. On the start of open-mitosis NE breaks down and all components of the NPC dispersed to the cytoplasm. At the end of mitosis, NE reforms and all the components are collected quickly to form the full NPC. This post-mitotic NPC reassembly is previously described to happen in an ordered stepwise process by starting with a seed nucleoporin structure. It has been previously reported that Y-complex components and Nup153 may be playing a role to initiate NPC formation according to observations made on mammalian cells by live fluorescence imaging. While this quick formation of NPC is also related to the accompanying membranal structure, the responsible mechanisms relating the membranal structures with possible seed nucleoporins for initiating the assembly of functional NPC remain unknown. To obtain direct evidence for this unknown problem, firstly I made high resolution observations on early telophase cells for membranal structures forming the NE by a method called as live correlative light and electron microscopy (Live-CLEM). As a result of these observations, sheet-like fenestrated endoplasmic reticulum (ER) membranes were found as precursors of NE. As an addition to this, first chromosome attached parts of these NE precursors were occupied with filled fenestrations similar to NPC while they had mostly empty fenestrations on the unattached parts. These results state a role for the importance of ER structure for NPC formation at the end of mitosis and fenestrations on ER membranes play a role on it. To clarify and show the importance of fenestrations on NPC formation, I used a novel experimental method including an artificial bead conjugated with a molecule of interest as an effector molecule to assemble the NPC. The beads were introduced into living cells and observed if the NPC, NE or their protein components are assembled at the effector molecules on the surface of the beads on post-mitosis. As a result of these experiments, it has been

revealed that Nup133 (a component of Y-complex) and Nup153 are not enough alone to create a full NPC molecule. However, Nup153 has been seen to interact with inter-subcomplex components of NPC more efficiently than Nup133. As an addition to this, it has been seen that both nucleoporins have the ability to collect NE-like double membrane and NPC-like structures under electron microscope with a different affinity for double layered membranes; Nup133 can collect double layered membranes more efficiently than Nup153 at the end of mitosis. Also, membranes in relation with Nup133 has higher number of fenestrations than Nup153. Because of the early accumulation of Nup133 around chromosomes and high affinity of it for fenestrated membranes, I introduce here that it can anchor double layered membranes possibly through these fenestrations residing on NE precursors while Nup153 can collect double layered membranes with the help of transmembrane nucleoporins. Because of these opposite affinities of Nup133 and Nup153 for membranes and nucleoporins, both of their role is possibly necessary for the quick assembly of NPC at the end of mitosis. As a result, it is introduced here that instead of a single seed nucleoporin, multiple nucleoporins are working together with membranes and also possibly with chromosomes in different roles to initiate and finish NPC formation post-mitotically.

Table of Contents

Abbreviations

NPC - Nuclear Pore Complex

NE - Nuclear Envelope

PBS - Phosphate Buffered Saline

PB - Phosphate Buffer

ONM - Outer Nuclear Membrane

INM - Inner Nuclear Membrane

ER - Endoplasmic Reticulum

FA - Formaldehyde

MeOH - Methanol

GA - Gluteraldehyde

BSA - Bovine Serum Albumin

EM - Electron Microscopy

Live-CLEM -Live-Correlative Light and Electron Microscopy

NA -Numerical Aperture

RT-PCR -reverse transcriptase polymerase chain reaction

SD - standard deviation

wt - wild type

AH- Amphipathic helix

ALPS- ArfGAP1 Lipid Packing Sensor

DMEM- Dulbecco's modified Eagle's medium

List of figures

Introduction

Nucleus is an organelle inside eukaryotic cells which includes genetic material covered and protected by a double layered membrane, nuclear envelop (NE). NE consists of two lipid bilayer membranes; inner nuclear membrane (INM) which is in direct contact with chromosomes by the help of INM transmembrane proteins and outer nuclear membrane (ONM) which is considered as being continuous with endoplasmic reticulum (ER). For the sustainability of life, instead of being fully protected from the environment, genetic material needs to be in contact with some proteins, RNAs and protein complexes. For example, mRNA transcripts created in the nucleus need to pass cytoplasm while the polymerases translated on the cytoplasm need to travel to nucleus to reach working destination. This limited and selective level of connection between nucleus and cytoplasm happens by the help of nuclear pore complexes (NPC). NPCs which perforate the NE by the joining of INM and ONM, are the main gates which ensure the necessary connection of nucleus with the cytoplasm. By being one of the biggest protein complexes inside the cell with its 125 megadalton weight in vertebrates (Reichelt et al., 1990), NPC consists of ~30 different proteins which are called as nucleoporins (Cronshaw et al., 2002). The 8-fold of these 30 nucleoporins creates an octagonal structure for NPC (Gall et al., 1967).

NE structure and function

NE as being continuous with the ER membranes has unique differentiations from the ER. ONM resembles to ER in protein composition. Thus, the differentiations are included mostly on the INM proteins which anchors the membrane and interacts with the chromosomes and nuclear lamina on metazoans. So far, there are more than 60 transmembrane proteins on INM also called as NETs and the function of the most are not investigated yet (Schirmer and Gerace, 2005). Mostly researched integral INM proteins are LBR, LEM-domain containing proteins

Lap2β, MAN1 and emerin. LBR is shown before to be able to bind to chromatin through heterochromatin binding protein (HP1) (Ye et al., 1997). Also, LEM domain containing proteins can also interact with chromatin through barrier to autointegration factor (BAF) (Segura-Totten et al., 2002; Gorjanacz et al., 2007). Also, NE proteins are direct interaction with the lamina. Nuclear lamina covers the INM and by interacting with some INM proteins stabilizes the nuclear membrane. Lamina includes a meshwork of A type and B type lamins.

As mentioned earlier NE is a barrier between cytoplasm and nucleoplasm, but as an addition to that, it also have role on various cellular functions. These functions are enabled by the help of INM proteins of NE mostly which include chromatin organization, regulation of gene expression etc. (Mattout e al., 2006; Heessen and Fornerod, 2007). As a functional and structural difference from ER, NE also includes nuclear pore complexes which are responsible for nucleo-cytoplasmic transport and the communication of cytoplasm with nucleoplasm.

NPC structure and function

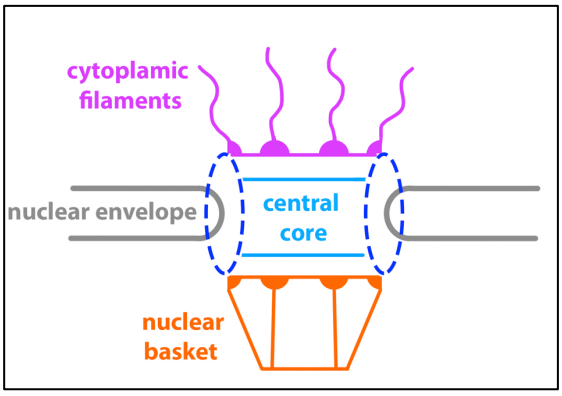

Figure 1. General structure of NPC

As shown in figure 1, NPC architecture can be divided into main 3 groups; cytoplasmic filaments, central core and nuclear basket. Some nucleoporins create sub-complexes by directly connecting and acting together with other nucleoporins (Schwartz, 2005). On figure 2, these subcomplexes are shown in same color with all other nucleoporins included in NPC.

Cytoplasmic filaments consist of Nup358(RanBP2), Nup88 and Nup214. Even though Nup88 is considered to contributing central channel components in direct transport (Grossman et al., 2012), it is classified as a cytoplasmic filament (Hurwitz et al., 1995). Cytoplasmic filaments

are reported as having roles on transport mechanisms (Hutten et al. 2009), mRNA export (Kramer et al., 1995), and even protein modification (Mahajan et al., 1997).

Central core is the main channel of the NPC and includes, scaffold nucleoporins, transmembrane nucleoporins, central scaffold spoke-ring nucleoporins and transport channel nucleoporins. Scaffold nucleoporins include the Y-complex (also called as Nup107-160 complex) components. Because of its Y-shaped structure under electron microscope, this sub-complex of NPC is called as Y-complex (Siniossoglou et al., 2000) and it consists of mainly 9 nucleoporins in vertebrate; Nup107, Nup160, Nup133, Nup96, Nup85, Nup43, Nup37, Seh1 and Sec13 (Neumann et al. 2010). This complex localizes to both sides of nuclear envelope on cytoplasmic and nuclear sides. As being different from cytoplasmic Y-complex, nuclear complex also includes ELYS nucleoporin which is sometimes mentioned as being a part of Y-complex (Rasala et al., 2006). Transmembrane proteins include Pom121, Ndc1, gp210 and TMEM33. These transmembrane proteins are thought as being the main anchors of NPC to the double layered NE (Mitchell et al., 2010). Central scaffold spoke-ring nucleoporins are Nup93 complex components. As being the second largest sub-complex, this sub-complex consists of Nup93, Nup155, Nup205, Nup188 and Nup35 (Vollmer and Antonin, 2014). Transport channel nucleoporins include multiple sub-complexes which are mainly responsible for selective transport of NPC. These sub-complexes are Nup62 complex and Nup98 complex. Nup62 complex consists of Nup62, Nup58, Nup54, Nup45 which are also called as FG-Nups (Hu et

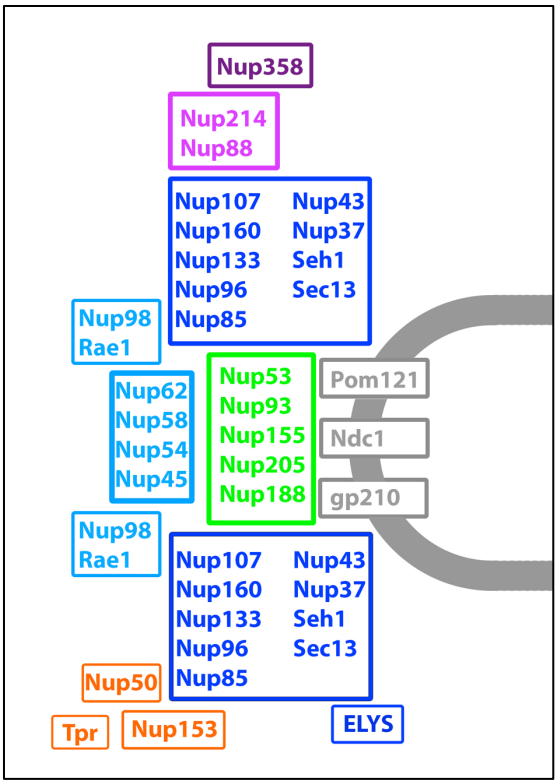

Figure 2. Components of NPC in metazoan. Subcomplexes are written in same color and enveloped by rectangles.

al.,1996). FG-Nups which include phenylalanine glycine repeat, have an intrinsically disordered structure (Bayliss et al., 2000) and they are thought as being responsible for main transport activity of NPC (Lim et al., 2007). One third of NPC components includes FG repeats.

Nuclear basket as being the last part to explain for NPC structure in this part, has Nup153, Nup50 and TPR as the main components. Previously, nuclear basket components are published as being important for mRNA export, telomere organization, spindle pole assembly, and non-spliced RNA retention (Bastos et al., 1996; Frosst et al., 2002; Xu et al., 2007). TPR is considered as the main structural component which creates the basket-like architecture on nuclear side of NPC (Krull et al., 2004). Nup153 is considered as the linker between TPR and the main core of the NPC (Krull et al., 2004).

The main function of NPC is considered as transport through cytoplasm and nucleoplasm. However, there are also several reports for NPC components to be involved in multiple nuclear functions other than transport. These functions include, gene regulation, chromatin organization, transcriptional memory and DNA repair (Zwerger et al., 2012).

NE and NPC on disease

NE is the main component protecting the genetic material in eukaryotes. Even though there is no direct evidence for the relation of post-mitotic NE formation with diseases, mutations on lots of the INM proteins having a role on NE reformation, cause diseases. Mutations on lamin proteins for example cause a set of diseases called as laminopathies. A-type lamins are coded by *LMNA* gene (Lin and Worman, 1993) and mutations in *LMNA* mainly effects striated muscles, adipose, and peripheral nerve and also causes progeria phenotype. Some examples for *LMNA* mutation caused diseases can be given as congenital muscular dystrophy (Quijano-Roy et al., 2008), Emery-Dreifuss muscular dystrophy (Bonne et al., 1999), Dunnigan-type familial partial lipodystrophy (Jackson et al., 1998; Peters et al., 1998), Charcot-Marie-tooth

disease type 2B1 (De Sandre-Giovannoli et al., 2002), and Hutchinson-Gilford progeria syndrome (Eriksson et al., 2003). As an addition to that, mutations on transmembrane INM proteins or NETs also causes a number of diseases called as nuclear envelopathies. These diseases include myopathies, progeria syndrome, and also some neurogenerative diseases too. As an INM protein, LBR is coded by the gene *LBR* and mutations in this gene causes a disease called as Pelger-Huet anomaly (Hoffman et al., 2002). Another INM protein emerin is coded from *EMD* gene and mutations on these genes also causes Emery-Dreifuss muscular dystrophy (Bione et al., 1994).

Similar to NE, dysfunctional NPC also causes diseases. Because of being the main gate interacting the cytoplasm with nucleoplasm, NPC should maintain its function properly to protect the cells from possible infections and diseases. Disfunction of NPC is related previously to neurological disorders, viral infections and also cancer (reviewed in Sakuma et al., 2017). Previously it has been shown that, unproperly formed NPC tend to lose their proper function and leaking products both side of the NE (D'Angelo et al., 2008). Also reduced levels of different components for NPC, causes serious diseases like leukemia (Lin et al., 2005; Iwasaki et al., 2005), tumorigenesis (Naylor et al., 2016), embryonic lethality (Smitherman et al., 2000; Okita et al., 2004), sudden cardiac death (Zhang et al.; 2008) etc...

Because of these importances, the correct formation of NE and NPC during cell cycle are important to maintain healthy life of a cell.

NE reformation at the end of mitosis

On metazoans NE breaks down in the start of mitosis and has to reform again at the end of it. To maintain the proper cell function, NE has to form quickly and correctly after each division. This kind of cell division is called as open mitosis. At the end of mitosis, NE forms from ER membranes around chromosomes. Recently it has been shown with high resolution electron

microscopy, different types of cells include structurally different ER membranes which are related to their roles in an organism; like secretion etc. (Puhka et al., 2012). And it has also been shown with EM, the structures of ER membranes tend to include more fenestrations and tubules during mitosis (Puhka et al., 2007). It is a subject of debate what kind of structural ERs initiating the first post-mitotic NE. There are several reports from different types of cells, claiming sheet-like, fenestrated or tubular ERs are the precursors of post-mitotic NE (Lu et al., 2011; Otsuka et al., 2018; Anderson and Hetzer, 2007). Tubular ER is a type of endoplasmic reticulum which has the shape of a tube-like structure with long and connected membranes. Besides that, sheet-like ER is the endoplasmic reticulum which has the structure of a continuous membrane with wide and long structure.

Recruitment of ER membranes to chromosome surface is thought to happen by the INM proteins. These chromosome interacting INM proteins include LEM domain proteins which interact with BAF DNA interacting protein (Segura-Totten et al, 2002; Gorjanacz et al, 2007), and also LBR which interacts with HR1 chromatin interacting protein (Ye et al., 1997). It has been previously shown that NE starts to form from the so called “non-core region” of the chromosomes which corresponds to more peripheral regions of chromosome mass. Transmembrane proteins like LBR, Lap2β starts to accumulate around these regions of chromosome mass in early telophase (Haraguchi et al., 2008). Except the LBR (Lu et al., 2010), there is no transmembrane NE protein which has shown to be essential for NE formation. The depletion of these proteins mostly causes late NE formation but does not inhibit the formation of it (Anderson et al., 2009).

NPC reformation mechanisms

NPC is shown to form in two distinguished mechanisms in open-mitosis cells. One happens during interphase where the NPC are formed on the intact double layer membrane of NE. And the other is post-mitotic which includes the reformation of broken NE together with NPC.

The main difference of interphase and post-mitotic NPC assembly is probably the structural difference between membrane which will reside the newly forming NPC. During interphase, a highly curved membranal gap should form on intact double layer NE to position the NPC inside of it. This process is considered to take place in more than 30 min (Dultz et al., 2010). Compared to interphase NPC assembly, post-mitotic functional NPC appears in around 10 minutes which is extremely quicker than interphase assembly (Dultz et al., 2008). The main reason for this rapid process is probably the effect of newly forming NE together with NPC on post-mitosis. Before the start of mitosis, INM proteins, lamins and also nucleoporins are phosphorylated by the help of kinases and this phosphorylation causes NE proteins together with the components of NPC to be dispersed to the cytoplasm (Champion et al., 2017) while causing a diffusion of NE to endoplasmic reticulum (ER) (Yang et al. 1997).

To define NPC assembly together with NE reformation, there are mainly two models proposed previously; insertion model and enclosure model (Shooley et al., 2012; Schellhaus et al., 2015). For insertion model, NE forms firstly by the expansion of tubular or sheet-like membranes around the chromosomes and NPCs are inserted to those intact double layer membranes similar to interphasic NPC assembly (Lu et al., 2011; Fichtman et al., 2010; Macaulay and Forbes 1996). When the quick formation of post-mitotic NPC considered, this model cannot explain the main difference between interphase and post-mitotic NPC assembly. Another model called as enclosure model claims the existence of pre-pore structures on chromosome surface (Sheehan et al, 1988; Burke and Ellenberg, 2002; Walter et al., 2003a). When the NE reforms from tubular or sheet-like ER, it expands and covers the pre-pore structures while enabling full

formation of NPCs in this model. The quick formation mechanism of NPC is better explained with this model in the case when NE forms from tubular ER or fenestrated ER sheets.

NPC assembly is proposed to happen in a stepwise process for the regulation of nucleoporins (Chaudhary et al., 1993; Bodoor et al., 1999; Haraguchi et al., 2000; Daigle et al., 2001; Belgareh et al., 2001). In this aspect, interphase and post-mitotic NPC assembly differentiate from each other by the first regulation of nucleoporins. Previously it's been reported that there are some important components of NPC playing significant roles as seed structures to form new NPC for both interphase and post-mitotic NPC assembly. Pom121 is shown as a key molecule to start new NPCs on interphase NE by its inner nuclear membrane localization (Doucet et al., 2010; Dultz and Ellenberg, 2010). On the other hand, ELYS, Y-complex and Nup153 are reported previously as being important as a starter of NPC on post-mitosis because of their early recruitments to chromosome surface after anaphase onset (Dultz et al., 2008; Daigle et al., 2001; Belgareh et al., 2001; Bodoor et al., 1999). Inside of them, ELYS nucleoporin which is reported to have an AT hook domain helping NPC to interact with DNA, is considered as an important starter molecule because of its interaction with Y-complex (Rasala et al., 2006; Franz et al., 2007). It is thought as a recruiter of Y-complex to chromosome surface in the first step. On previously reported models, these molecules are considered as the components of seed structure and by the help of them other components start to collect by the addition of membranes with the help of transmembrane nucleoporins like Pom121. Single roles of these possible pre-pore components on membrane interaction post-mitotically is an issue of interest with no published data.

Nup133

Nup133 is a member of Y-complex. There are two important structural domains of Nup133; N-terminal and C-terminal domain. Its direct interaction with Nup107 through its C domain

has been shown before (Boehmer et al., 2003; Berke et al., 2004). Nup133 also has been reported to interact with kinetochores during mitosis together with the other components of Y-complex (Belgareh et al., 2011). After anaphase onset, Nup133 starts to accumulate around chromosomes earliest compared to the other components of NPC (Dultz et al., 2008; Belgareh et al., 2001). Because of this early localization Nup133 is considered as being one of the most important NPC assembly starters on post-mitosis (Walter et al., 2003a; Dultz et al, 2008). As an addition to this, it is shown in LacO/LacI assay that Nup133 can collect most of the nucleoporins (Schwartz et al., 2015). N-terminal domain of Nup133 includes a small polypeptide chain (23 amino acids) with a function similar to amphipathic helices (AH) and this domain is called as ALPS (ArfGAP1 Lipid Packing Sensor) motif (Begay et al., 2005). A null ALPS motif existence on Nup133 causes a cytoplasmic localization and also shows a lack of NPC formation during interphase (Doucet et al., 2010). Interestingly these cytoplasmic localized mutants, localize to NEs during anaphase which suggests cell cycle dependent function for ALPS domain of Nup133 (Doucet et al., 2010). Because of these interesting features of Nup133, the effect of it on NPC formation after mitosis in relation with membranal structures may give interesting results.

Nup153

Nup153 is considered as important because 10% of it firstly accumulate around chromosomes much earlier than other nucleoporins after anaphase onset (Dultz et al. 2008; Bodoor et al.., 1999; Belgareh et al., 2001). This early regulation of it, suggesting a possible role for post-mitotic NPC formation. Nup153 is also shown previously as recruiting most of the NPC components to nuclear periphery according to LacI/LacO array (Schwartz et al., 2015). It has been previously shown that for recruitment of Nup153 to NPC, TPR, Nup98, Nup93 and Nup205 are not required (Wu et al. 2001, Hase and Cordes 2003), while Y-complex is

necessary (Boehmer et al. 2003; Krull et al. 2004; Walther et al. 2003). Nup153 is reported to bind Y-complex through its N-terminal domain (Vasu et al. 2001; Walther et al. 2003).

Nup153 is a nuclear basket protein. It consists of mainly three structurally important domains; N-terminal domain, central domain which has multiple zinc finger motifs and also C-terminal domain with multiple FG repeats (Ball and Ullman, 2005). N terminal domain is reported as being important for NE localization (Bastos et al. 1996; Enarson et al., 1998). N terminal domain includes an amphipathic helix (AH) with 18 amino acids in total, and with the help of this sequence Nup153 considered to be interacting with membranes (Vollmer et al., 2015). AHs are included in lots of membrane related proteins, and they are considered as being important for membranal recognition and modification (Grin and Anthony, 2010). AHs have hydrophobic and polar residues in two opposite faces of the α-helix which helps them to bind membranes. These helices showed before to remodel membranal structures (Ford et al., 2002). Nuclear basket proteins Nup1 and Nup60 (orthologs of Nup153) in S. cerevisiae, also have AH structure. Overexpression of AH including N terminal domains of Nup1 and Nup60 created highly curved NE compartments in-vivo and also their binding and deforming abilities for membranes shown previously (Meszaros et al., 2015). As a result, they are suggested to regulate membrane curvature. As an ortholog of them, Nup153 also includes an AH, which creates intriguing questions for its affinity and ability to bind and modify membranes.

Live correlated light and electron microscopy (Live-CLEM)

Dynamic structures in living cells are generally observed by fluorescence microscopy, but this method lacks the high-resolution structural information. To obtain detailed structural data, fluorescence microscopy has been joined with the electron microscopy and CLEM (Correlative Light and Electron Microscopy) method has been created (Nakata et al.1998). When a live imaging is joined with CLEM a method called as ‘Live CLEM’ is invented (Haraguchi et al.,

2015). In this technique, cells with proteins tagged fluorescently are observed live with fluorescence microscopy and fixed in desired time points (Fig. 3). Fixed cells are prepared for electron microscopy (Fig. 3). By correlating the live and fixed fluorescence results with electron microscopy results, a molecular specific high-resolution image can be obtained from a dynamic point of view in the context of cell structure. Live CLEM has been used in this study as the main method.

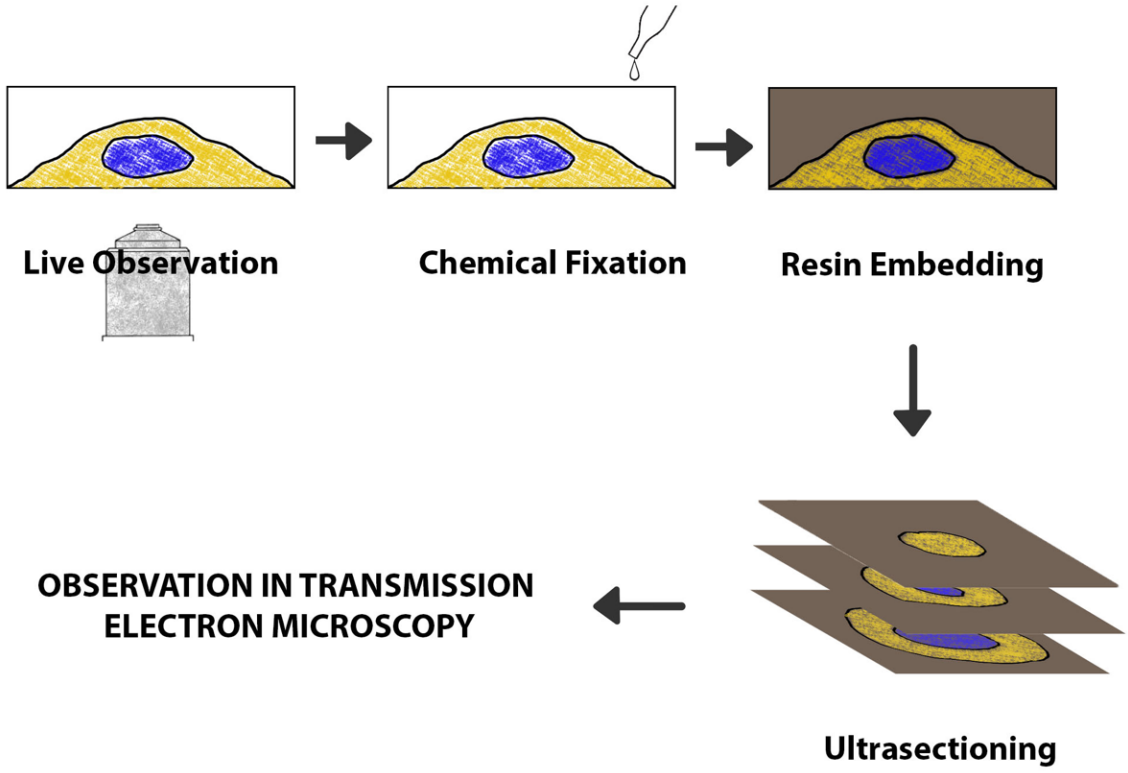

Figure 3. General live correlative light and electron microscopy (Live-CLEM) scheme.

In-vivo bead insertion method

It is a common experimental procedure to use DNA-beads and protein conjugated beads inside of xenopus egg extracts. Because of being an invitro experiment and also limitations this method has differentiations from in-vivo experiments. To prohibit these limitations a new method to insert beads inside of living cell has been discovered (Kobayashi et al., 2010). Beads are inserted inside of cells by the help of commercially available transfection reagents and these

beads are taken inside of cells with endocytosis (Kobayashi et al., 2010). After endosomal membrane is broken down, bead is facing with the cytoplasm. After they face with cytoplasm, they are attacked by autophagy (Kobayashi et al., 2010). Bead can escape from autophagy if its conjugated with cell life related materials. Previously it has been shown that DNA covered beads can escape autophagy (Kobayashi et al., 2015). Similar to these, GFP antibody conjugated beads can be used inside of "GFP conjugated protein of interest" expressing cells. When the endosomal membrane is broken and the bead is faced with the cytoplasm, the protein of interest will start to accumulate around the bead with the help of the interaction between GFP on protein and anti-GFP on the surface of bead. This way beads can be used as an artificial reaction templates to investigate intracellular interactions of specific molecules in living cells (Kobayashi et al., 2010). In figure 4 this procedure is summarized.

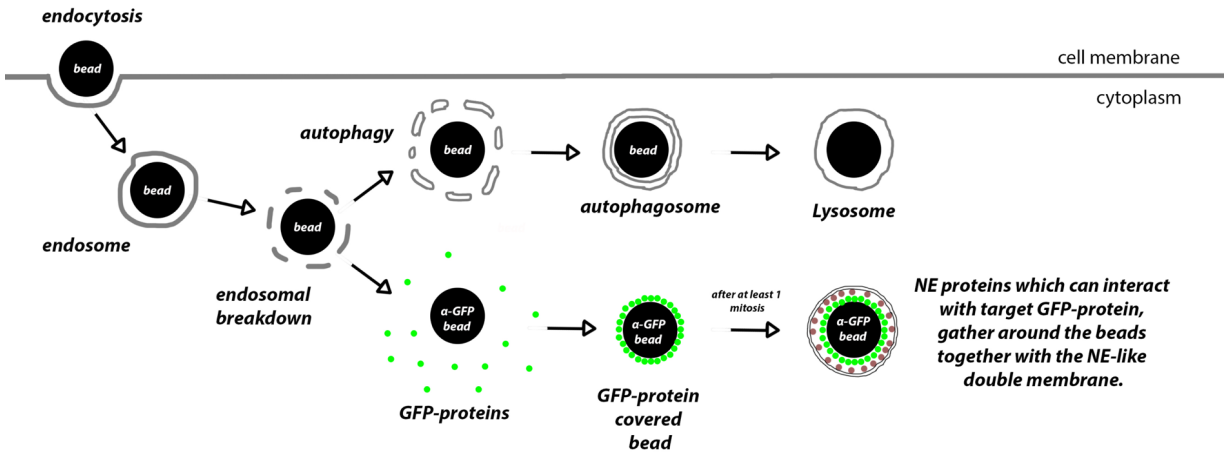

Figure 4. A general pathway for a bead entering to cell

For this thesis, GFP antibody conjugated beads are used and they are inserted inside of EGFP-Nup133 and EGFP-Nup133 stably expressing cell lines.

Aims and objectives

Previously it has been shown that, unproperly formed NPC tend to lose their proper function and leaking products both side of the NE (D'Angelo et al., 2008). And disfunction of NPC is related previously to neurological disorders, viral infections and also cancer (reviewed on Sakuma et al., 2017). Because of these effects of NPC, the correct formation of it during cell cycle is important to maintain healthy life of a cell.

There are multiple models to explain post-mitotic NPC assembly, but none of them shows clear explanations for the first relation of NPC components with NE precursors. The research made to show single roles of NPC components in-vivo on post-mitosis without the effect of chromosomes is limited. Earlier assembly of Nup133 and Nup153 around chromosome on mitotic exit, suggests an important role for them both in post-mitotic NPC assembly process. Also, there are several reports for their interactions with membranes. However, the importance of their membrane interactions is not investigated on post-mitotic NPC assembly. In this report, intracellular interactions of Nup133 and Nup153 tried to be examined on post-mitotic cell stage by the help of in-vivo bead insertion assay by relating them with the structure of NE-precursors.

Materials and Methods

Cell lines

HeLa cells (Riken Cell bank, Tsukuba, Japan) maintained in Dulbecco's modified Eagle's medium (DMEM) supplemented with 10% calf serum in a CO_2 incubator (5% CO_2) at 37°C. HeLa cell lines stably expressing EGFP-BAF (designated as HeLa/GFP-BAF; Haraguchi et al., 2008) were maintained in DMEM medium containing 10% fetal bovine serum (FBS). Stable HeLa cell lines were obtained by the help of DNA plasmids encoding EGFP-Nup133 and EGFP-Nup153 and also Effectene transfection reagent (QIAGEN, 301425, Hilden, Germany) by following the manufacturer's instructions. Stable cells were selected in the presence of 800 μg/mL geneticin (Life Technologies, 11811-031, Carlsbad, CA, USA). DMEM 10% FBS was used to maintain transiently EGFP3xNup107, EGFP3-Nup153, Pom121-EGFP3 expressing and stably EGFP-BAF, EGFP-LBR, EGFP-Nup133, EGFP-Nup153 expressing cell lines.

Plasmid construction

By the help of TRIzol Reagent (Thermo Fisher Scientific, 15596026, Waltham, MA, USA), total RNA fraction for Nup133 and Nup153 was collected from HeLa cells. By using SuperScript III First-Strand Synthesis System (Thermo Fisher Scientific, 18080051, Carlsbad, CA, USA), their coding regions are amplified and inserted into SuperScript plasmid. Then, the generated DNA fragment encoding Nup153 and Nup133 was PCR-amplified respectively, using the following primer sets and inserted into the PB-EF1α-EGFP-MCS-IRES-Neo-C vector (System Biosciences, PB533A-2, Mountain View, CA, USA): the primer sets were EGFP FWD EcoRI InF PiggyBac (tctagagctagcgaattatggtgagcaagggcgaggagct) and hsNup153 REV EcoRI InF piggyBac (tccgatttaaattcgaattttatttcctgcgtctaacagcagt) for Nup153, and EGFP FWD EcoRI InF PiggyBac (tctagagctagcgaattatggtgagcaagggcgaggagct) and hsNup133 REV

EcoRI InF piggyBac (tccgatttaaattcgaattttatatttgtccctgaacataat) for Nup133.

To generate DNA plasmids encoding 3xEGFP (three tandem repeats of EGFP)-tagged proteins (3xEGFP-Nup153), we first constructed the pEF1-EGFP-C1 vector by replacing the CMV promoter of pEGFP-C1 (Invitrogen, PT3028-5) with an EF1α promoter, and then constructed the pEF1-3xEGFP-C1 vector by inserting two fragments of EGFP that had been PCR-amplified from the pEGFP-C1 vector using the following primer sets: the first primer set (set1) was EGFP3-C SGLGS FWD1 Kpn2I InF (agctgtacaagtccggactgggcagcatggtgagcaagggcgaggagct) and EGFP3-C SGLGS REV1 InF (agatcccaatccagacttgtacagctcgtccatgcc), while the second primer set (set2) was EGFP3-C SGLGS FWD2 InF (tctggattgggatctatggtgagcaagggcgaggag) and EGFP3-C REV2 Kpn2I InF (tcgagatctgagtccggacttgtacagctcgtccatgc). The DNA fragment encoding Nup153 was PCR-amplified from the pNup153 vector as described above and inserted into the pEF1-3xEGFP-C1 vector.

The DNA plasmid encoding Pom121-GFP was a kind gift from Dr. Naoko Imamoto (Riken, Japan). The DNA fragment encoding Pom121 was PCR-amplified from the pom121A-Venus plasmid (a kind gift from Dr. Naoko Imamoto, Riken) and inserted into the pEF1-3xEGFP-N1 vector. The DNA plasmid encoding lamin B receptor-EGFP (LBR-GFP) was described previously (Haraguchi et al., 2000).

Live cell imaging

The cells were seeded into 35-mm glass-bottom culture dishes (MatTek) at a concentration of 1.5×10^5 cells/dish and incubated for approximately 1 day before observation. At least 2 h before imaging, the medium was exchanged with pre-warmed fresh visualizing medium without phenol red supplemented with 10% FBS, 25 mM HEPES (pH7.3), and 80 μg/mL kanamycin. Images were acquired with an Olympus oil-immersion objective lens (UApo40x, NA = 1.35, Tokyo, Japan) with the DeltaVision Core microscope system (Applied Precision,

Issaquah, WA, USA) in a temperature-controlled room (37°C) as described previously (Haraguchi et al., 1999). The collected data was computationally processed by the ND-SAFIR denoising software (Boulanger et al., 2010).

The fluorescence intensity quantifications were made for the chromosome and nuclear rim areas for dividing cells. By accepting the time point before first separation of chromosomes, as 0, in every 1minute average fluorescence intensities were measured around chromosomes by the help of ImageJ (Schindelin et al., 2012). The used constructs for this quantification was; EGFP3-Nup107, EGFP-Nup133, EGFP-Nup153, Pom121-EGFP3 and EGFP-LBR. Multiple data obtained for each construct, normalized and averaged for every time point. Averaged results were graphed.

Anti-GFP Bead insertion

Cells were cultured in $1.5x10^5$ cells per plate to glass bottom 35 mm dishes (MatTek, Ashland, MA, USA). After one day incubation in 37°C, bead insertion was made by the help of Effectene transfection kit (QIAGEN, Germany) by excluding "enhancer reagent" from the kit (Kobayashi et al., 2015). Commercially available GFP antibody conjugated magnetic beads (MBL, D153-11 and D153-9, Nagoya, Japan) in 2 different sizes (1.6 μm and 3 μm in diameter) were used. After 2 hours of incubation of cells with bead + Effectene mixture on 37°C CO_2 incubator, bead solution was washed from cells with maintenance medium. After 24 hours of incubation on 37°C CO_2 incubator, cells including GFP positive signal beads were used for forward experiments. Theoretically, it is expected that, when the anti-GFP beads are inserted inside of the cells, if the endosomal membrane is broken, they will be covered by the GFP-protein which is expressed from the cell and also all the other related structures of GFP-protein. By this way, it will allow us to visualize and investigate intracellular connections in living cells. A diagram for the main experimental scheme used in this project can be seen on figure 5 and 6.

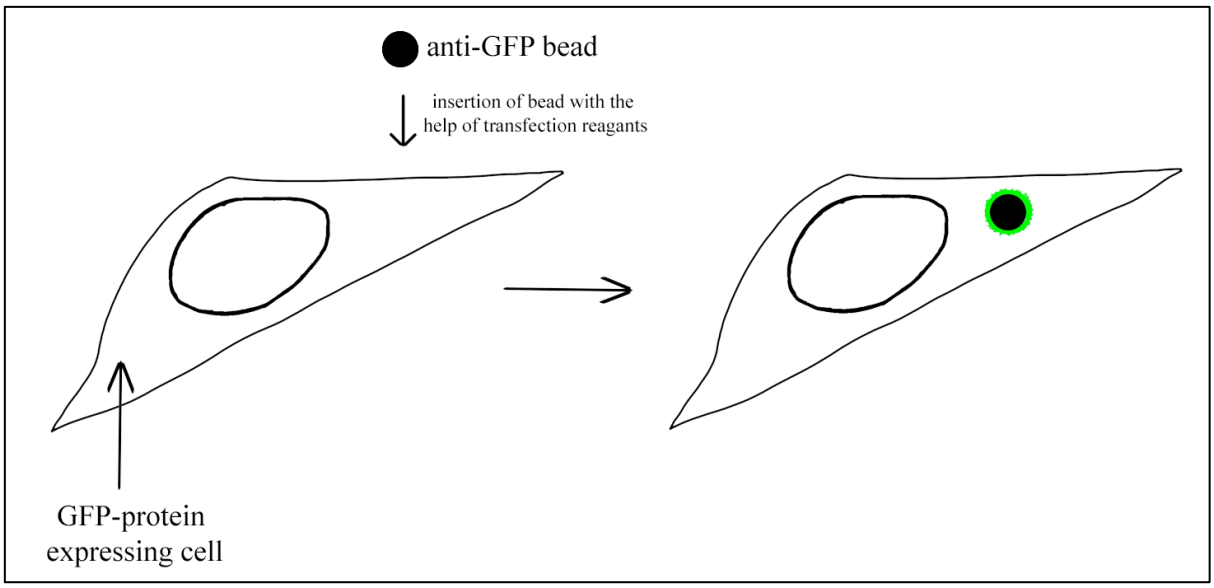

Figure 5. General logic of bead insertion method

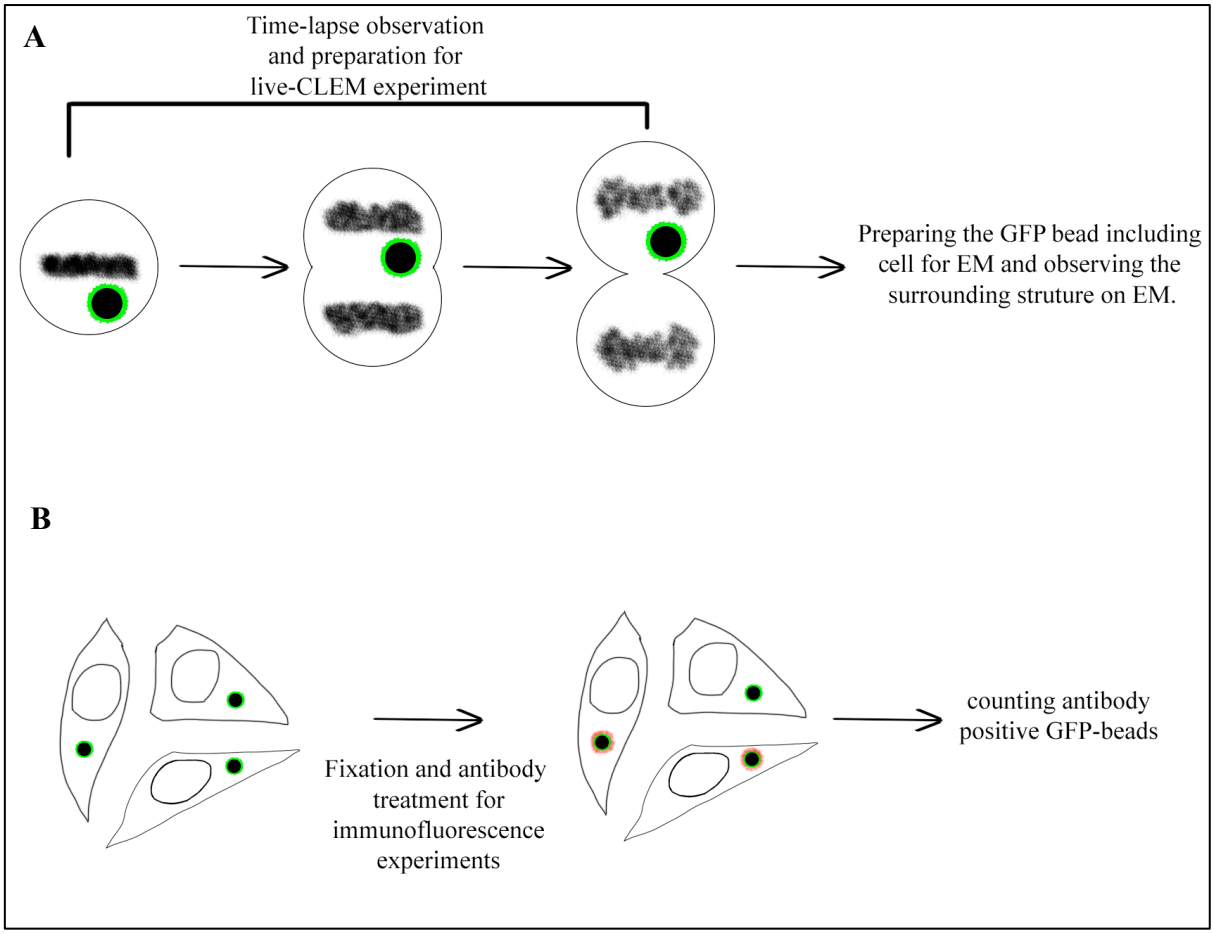

Figure 6. After inserting the beads, cells are used in live-CLEM imaging (A) or in immunofluorescence imaging (B) to reveal the protein or membrane interactions of proteins.

Immunofluorescence Staining

For immunofluorescence staining, cells were fixed with formaldehyde (FA) or methanol (MeOH). For FA fixation, cells were incubated 15 min with FA in 3.7% last concentration and treated with 0.1% Triton-X for 5 min before bovine serum albumin (BSA) and primary antibody treatment. For MeOH fixation, cells were incubated with 100% MeOH for 15 min before BSA and antibody treatment. Between each treatment, cells were washed briefly with phosphate buffer saline (PBS). After fixation reagent treatment, all cells for both fixation method were treated with 1% BSA for 1h and then with different concentrations of primary antibodies.

The following antibodies were used in this study: mouse monoclonal antibodies are mAb414 (Covance, MMS-120R, Princeton, NJ, USA), anti-TPR (Matritect, M1200), anti-Nup88 (Santa Cruz Biotechnology, sc-136009, Dallas, TX, USA), and anti-LAMP-1 (Santa Cruz, sc-20011). Rabbit monoclonal antibodies were anti-Nup133 (Abcam, ab155990, Cambridge, UK), anti-Nup62 (BD Biosciences, 610497, Franklin Lakes, NJ, USA), and anti-Ran (Abcam, ab155103). Rabbit polyclonal antibodies were anti-ELYS (Abcam, ab14431), anti-Nup107 (Novus Biologicals, NBP1-76926, Littleton, CO, USA), anti-Nup153 (Abcam, ab84872), anti-Pom121 (Novus Biologicals, NBP2-19890), and anti-RanBP2 (Abcam, ab64276). Affinity purified anti-Nup98 polyclonal antibody was prepared as described previously (Iwamoto et al., 2013). Alexa Fluor 594-conjugated and Alexa Fluor 555-conjugated secondary antibodies (goat anti-mouse IgG, goat anti-rabbit IgG) were purchased from Invitrogen (Carlsbad, CA, USA). The used concentrations of primary antibodies and used secondary antibodies are listed on table below with the fixation method for specific antibodies.

Table 1. Antibody list

Primary Antibody	Primary antibody Dilution	Fixation method	Secondary Antibody
Nup107 (Novus, NBP1-76926)	400x	FA	Rabbit Alexa594 (molecular probes, A11037)
ELYS (abcam, ab14431)	500x	MeOH	Rabbit Alexa594 (molecular probes, A11037)
Nup133 (abcam, ab155990)	100x	FA	Rabbit Alexa594 (molecular probes, A11037)
TPR (Matritect, M1200)	500x	FA	Mouse Alexa 555 (molecular probes, A21424)
Nup153 (abcam, ab84872)	200x	FA	Rabbit Alexa594 (molecular probes, A11037)
mAb414 (Covance, MMS-120R)	500x	FA	Mouse Alexa 555 (molecular probes, A21424)
Nup98 (Iwamoto et al., 2013)	500x	FA	Mouse Alexa 555 (molecular probes, A21424)
Nup62 (BD biosciences, 610497)	500x	FA	Rabbit Alexa594 (molecular probes, A11037)
Pom121 (Novus, NBP2-19890)	500x	MeOH	Rabbit Alexa594 (molecular probes, A11037)
RanBP2 (abcam, ab64276)	500x	FA	Rabbit Alexa594 (molecular probes, A11037)
Nup88 (Santa Cruz, sc-136009)	500x	FA	Mouse Alexa555 (molecular probes, A21424)
Lamp1 (Santa Cruz, sc-20011)	100x	FA	Mouse Alexa555 (molecular probes, A21424)
Ran (abcam, ab155103)	500x	FA	Rabbit Alexa594 (molecular probes, A11037)

Quantification of immunofluorescence results

The number of antibody positive and antibody negative beads were counted for each EGFP-Nup133 and EGFP-Nup153 positive beads inside cells. Experiments were repeated three times.

For each experiment the total number of GFP positive beads were normalized to 100 and the percentage of antibody positive beads to all GFP positive beads were calculated. All ratios from 3 experiments were averaged and the graphs were created with error bars (standard deviations).

Live-CLEM

One day after bead insertion, cells are dyed with Hoechst33342. Time-laps images of bead inserted cells were taken on Olympus oil-immersion objective lens UApo/340 (40x, NA=1.35) on the DeltaVision Core microscope system (Applies Precision) in 37°C temperature-controlled room. After cells started to divide, they were fixed on 1h or 15min after anaphase onset with 2.5% glutaraldehyde (final concentration) for 1h. After 1h, cells washed with PBS and three-dimensional images at 0.2 μm intervals were taken using an Olympus oil-immersion objective lens PlanApo (60x, NA=1.4). The same cells were prepared for transmission electron microscope (TEM). For this, they were post-fixed with 1% OsO4 (Nisshin EM, Tokyo, Japan) in phosphate buffer (PB), pH 7.4, for 1h, washed briefly with distilled water, and stained with 2% uranyl acetate in water for 1h. After washing briefly with water again, cells were sequentially dehydrated with 30%, 50%, 70%, 90% and 100% ethanol. Then the dehydrated cells were embedded in epoxy resin. For this, they firstly were incubated with 10%, 30%, 50%, 70% (v/v) Epon812 (TAAB, Berkshire, UK) in ethanol for 3 min, 90% Epon812 for 10 min, and 100% Epon812 for 1h. After overnight incubation with fresh 100% Epon812, cells again were treated with fresh 100% Epon812 for 3h. Then, they were embedded in epoxy by incubating them with 100% Epon812 in 60°C for 2 days. The epoxy block was trimmed and ultra-sectioned with a thickness of 80 nm using a microtome (Leica microsystems, Wetzlar, Germany). Thin sections were stained with 2% uranyl acetate (Merck, Billerica, MA, USA) for 15 min and lead citrate (Sigma, St. Louis, MO, USA) for 1 minute. Image data were collected using an electron microscope JEM1400 in 80 kV (JEOL, Tokyo, Japan) with Digital Micrograph software (Gatan, Inc., Pleasanton, CA, USA).

Quantifying the length of membranes, the number of NPCs and fenestrations, also distance of membranes to bead surface

The membrane lengths were measured for the inner surface of the double layer membrane by using ImageJ (Schindelin et al., 2012). To see ratio of membrane length to membrane surface length, middle 10 serial sections of each bead were used. To count the number of NPC-like structures and fenestrated structures, 10 middle serial sections were used with 1 section intervals not to cause multicount for them. Total NPC amount and also fenestration amount is counted and calculated per 10 μm membrane for 3 different samples and graphs are created with the average of all 3 by including error bars (standard deviations).

The distance between the bead surface and membrane was measured as follows. First, the geometrical center of the bead was determined by using ImageJ software, and then the distance was measured automatically with ImageJ software along the lines radiating from the center (see Fig. 7A). The distance from the bead center to the surface of the inner membrane was determined as “a”, while the distance from the bead center to the surface of the bead was determined as “b”. The difference between a and b was determined by subtracting “b” from “a” to obtain the distance (see Fig. 7B). Distance was measured for 25–30 angular positions in a single TEM image, which was repeated for the middle 4 ~5 TEM section images to produce approximately 100 to 150 values for each single bead. The distance was calculated by averaging all values for each bead. The mean and standard deviation of the distance were determined from three different beads.

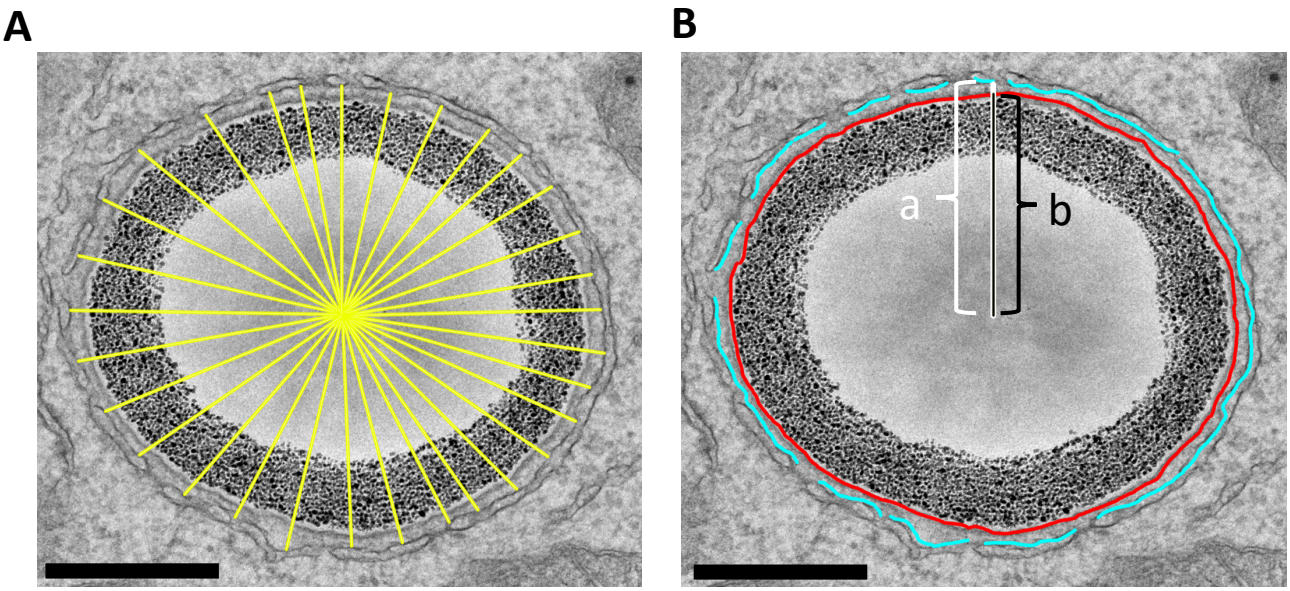

Figure 7. Membrane distance measurement. A is a representative image showing the center of the bead with the ~30 angular positions measured for this section. On B, bead surface is indicated with red colored line and inner surface of the membrane is indicated with cyan colored line. “a” indicates the distance of bead center to the inner membrane, “b” indicates the distance of bead surface to bead center.

Results

Nuclear envelope (NE) reforms from fenestrated sheet-like ER

To investigate NE reformation around chromosomes, firstly the cells in early telophase or late anaphase stage of cell division has been observed by live-CLEM imaging. For this, EGFP-Nup153 transiently expressing cell has been observed in every 1 min and fixed with GA when the first accumulation was observed around chromosomes. Nup153 has been previously reported to localize around chromosomes really early (Bodoor et al.., 1999; Belgareh et al., 2001; Dultz et al., 2008) and because of this reason Nup153 has been used. Fixed cell has been prepared for TEM in 100 nm serial sections. 8 serial section from the cell has been used and modelled to see the general structure of ER membranes forming the NE. Live-imaging and also fixed EM images can be seen on figure 8A and B and serial sections used for modelling are also shown on figure 8C and D. According to modelled data from these 8 serial sections corresponding to 800 nm thickness of membrane, it has been clearly observed that, NE starts to form from sheet-like ER membranes by attaching firstly to the non-core region of chromosomes (non-core region is defined as a region of telophase chromosome mass distant from the mitotic spindle attaching region; Haraguchi et al., 2001) (Figs. 8 and 9). This result is consistent with some previously made observations about NE starts to form from the non-core region of chromosomes (Haraguchi et al., 2008) and also it forms from sheet-like ER membranes (Lu et al., 2011).

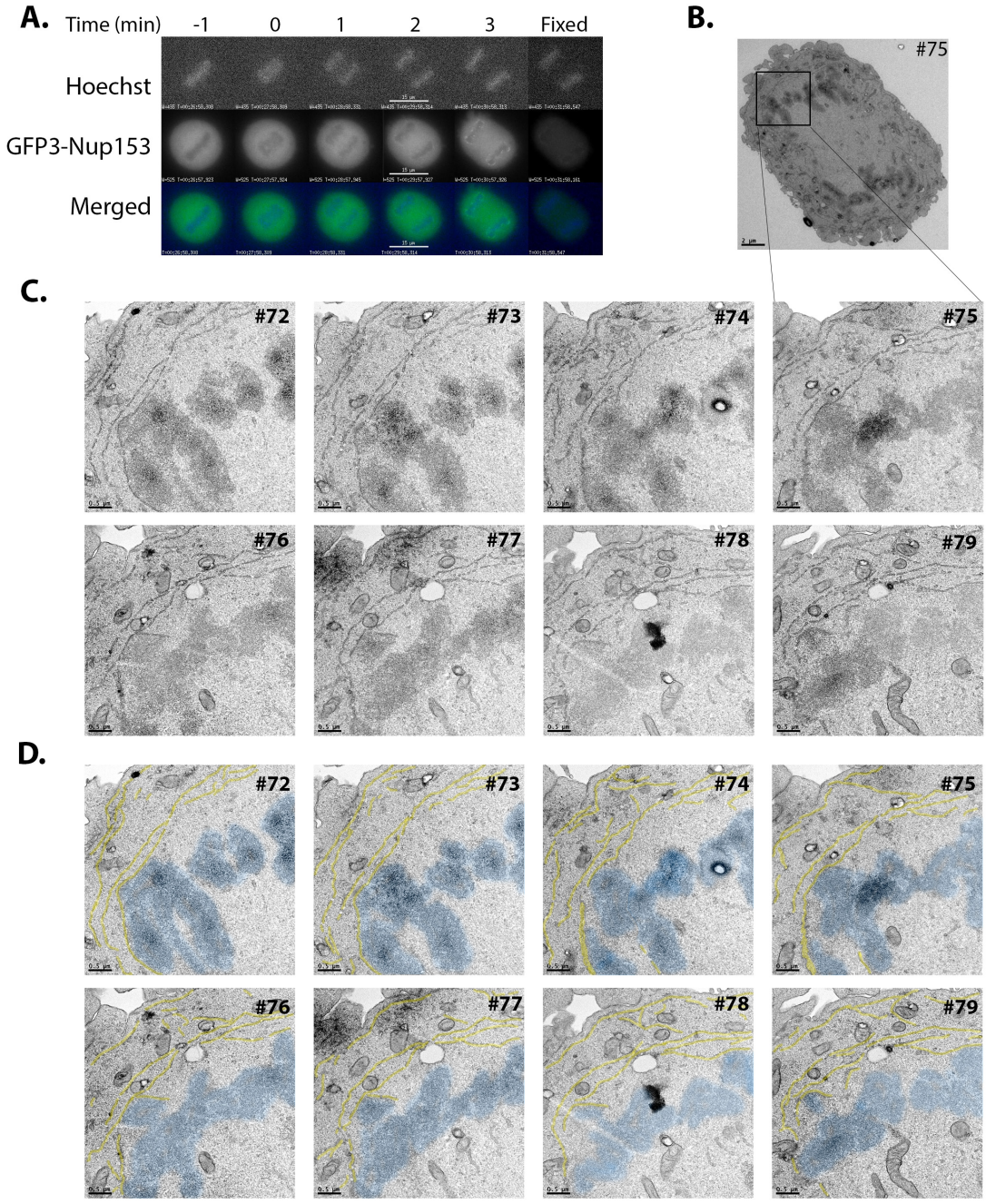

Figure 8. Nuclear envelope forms from sheet-like ER in HeLa cells. A. Time-lapse image of GFP3-Nup153 transiently transfected dividing cell. Merged image represents chromosomes (blue) and GFP3-Nup153 (green). 0 min corresponds to first time point of anaphase onset. B. Low magnification EM image of the same cell in A. C. Following serial sections with same following ER-NE membranes. D. Colored images for C, yellow for ER-NE membranes, blue for chromosomes. (This sample contains 131 sections in total and between 72 and 79 sections are represented here. Each section is in 100 nm thickness.)

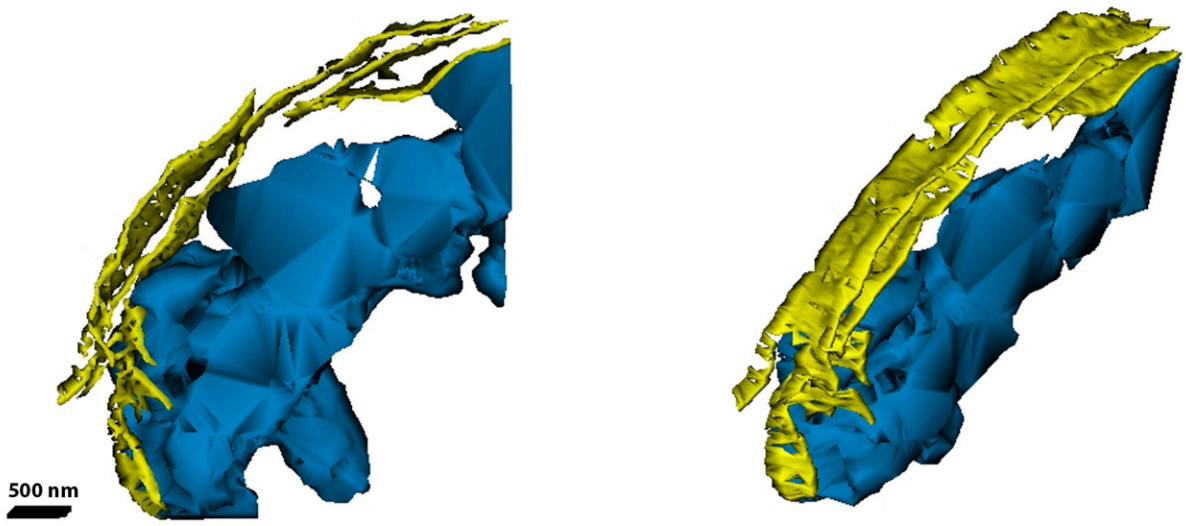

Figure 9. Sheet-like ER was observed clearly in reconstructed image of serial sections. Yellow parts show the membranes which are forming the nuclear envelope, blue parts show the chromosomes. This image has been obtained from serial sections shown in Fig. 8C and D with the help of "Reconstruct" software product.

Previously in different cell types, an increased amount in fenestrated sheets and tubular ER during metaphase has been reported by the modelled serial sections from TEM (Puhka et al., 2012). To examine the existence of these fenestrated sheets on anaphase, and whether the fenestrated membranes are involved in NE reformation, I used live CLEM imaging technique again. For this, firstly, GFP-BAF expressing HeLa cells were observed time-lapse on fluorescence microscopy and then fixed with GA a few minutes after anaphase onset as explained in methods section. At a time point when GFP-BAF signal was not localized to the NE, on 4th min after anaphase onset, cells are fixed and prepared for TEM. In this time point, high amount of fenestrated ER sheets was observed really near to chromosome mass from the non-core regions (Fig. 10). The fenestrations in different size on sheet membranes are shown in red dots (Fig. 10C'-D'). Similar results have been obtained for 4 different cells having different NE or NPC markers as LBR and Nup153.

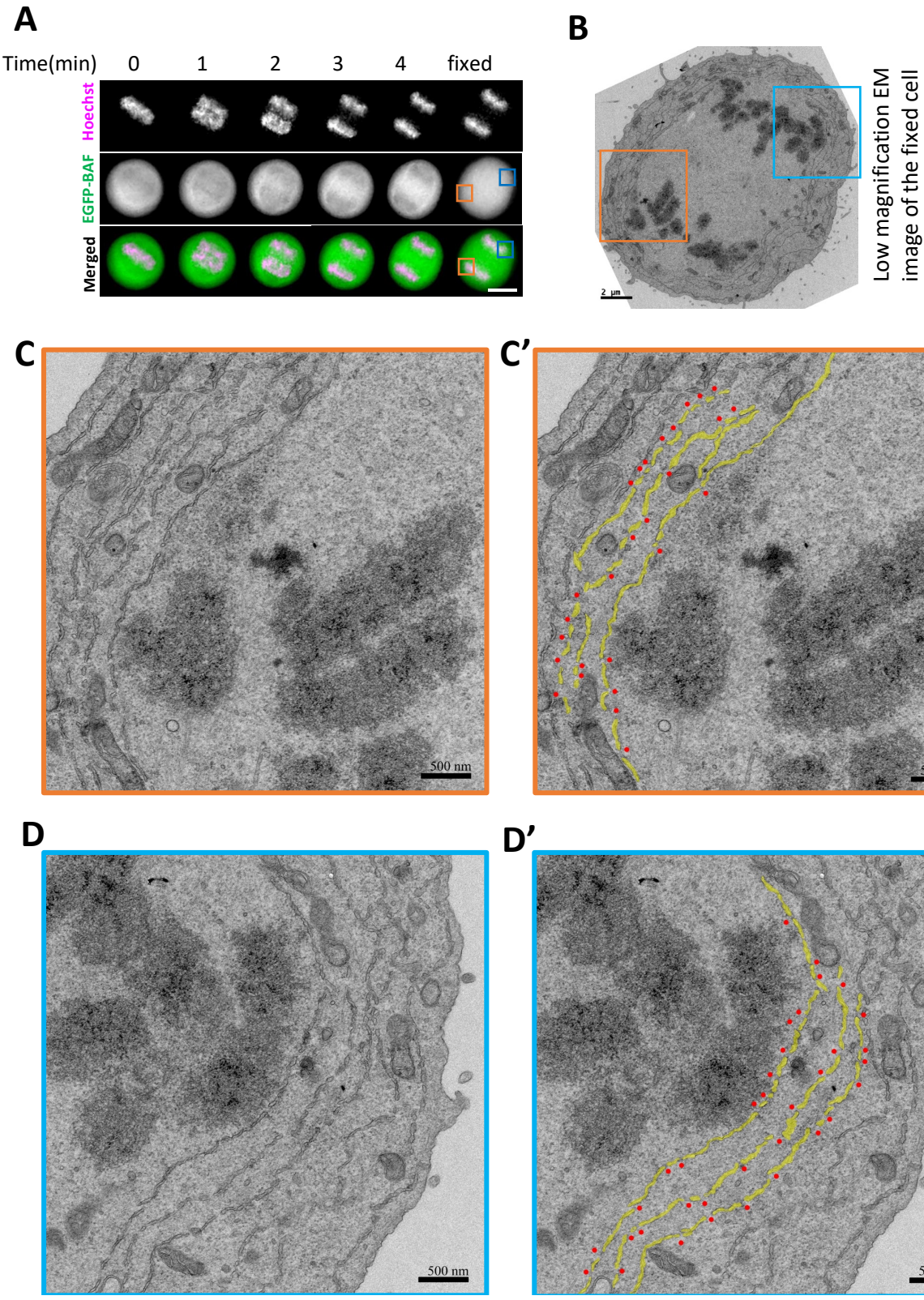

Figure 10. Existence of fenestrations on membranes so close to chromosomes for anaphase cells. (A) Time-lapse fluorescence image of the fixed cell with EGFP-BAF expression. Scale bar is 10 μm. (B) Low magnification EM image of the same cell. High magnification images of orange square (C) and blue square (D) on B, are colored with yellow for membranes (C', D'). fenestrations are indicated with red dots.

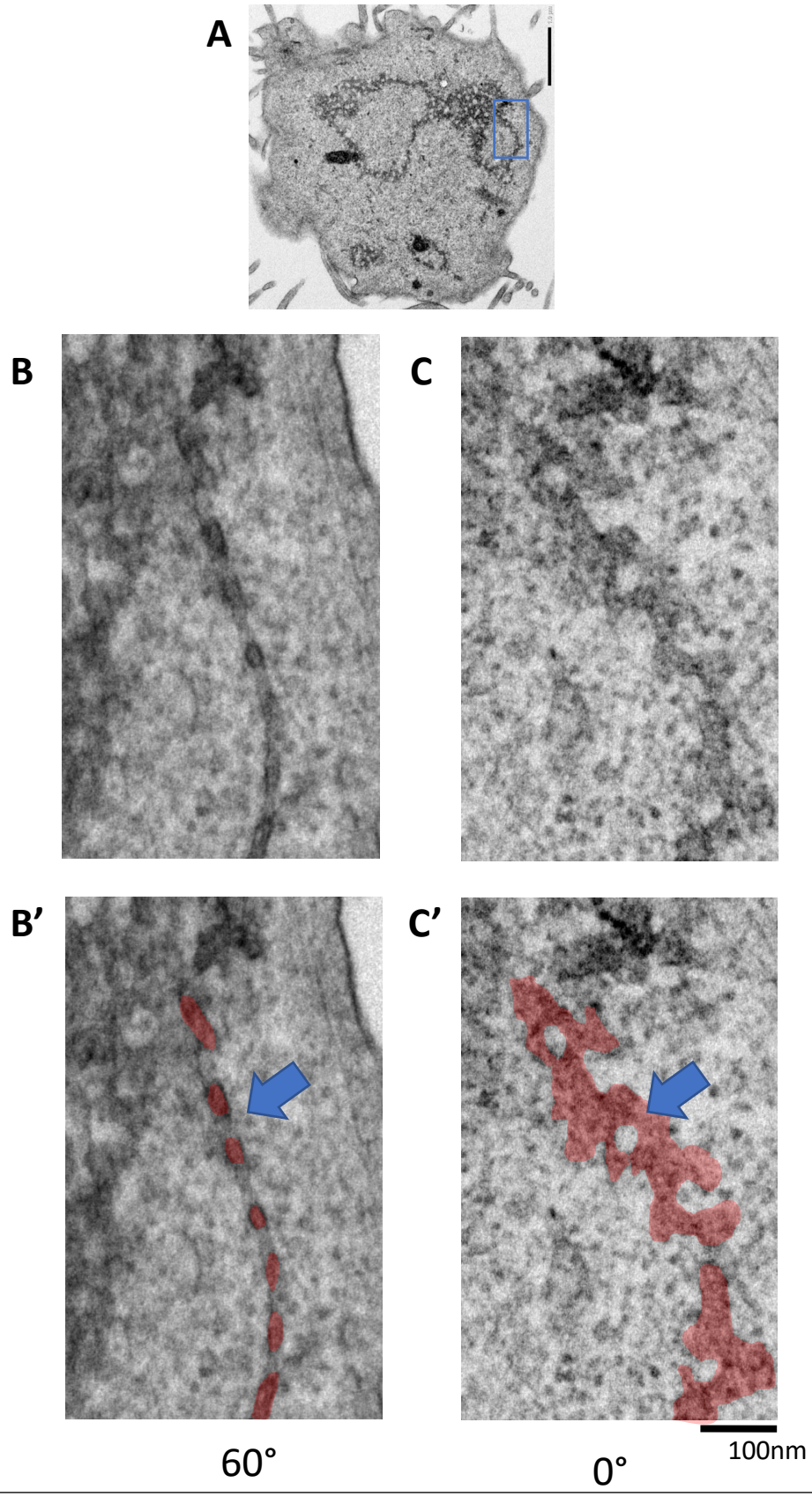

Figure 11. During metaphase too ER membranes includes lots of fenestrations. A is a top view of a metaphase cell, lots of circler empty looking fenestrations are visible. C is the high magnification view of the blue square in A. B is the 60° tilted image of the C. colored images can be seen on B’ and C’ for B and C’. Blue arrow is showing the same fenestration.

As an addition to telophase cells, to confirm the earliest existence of fenestrated ER membranes during mitosis, I also took images of metaphase cell on EM. According to these observations also lots of fenestrated empty looking structures were observed on ER membranes inside metaphase cells (Fig. 11).

Fenestrated membranes start to be filled on chromosome attached parts with structures similar to NPC

To prove that these fenestrated ER membranes are used as an NE precursor, samples from anaphase or early telophase cell stage with some NE or NPC related signals were used with similar experiments. Nup153 which is one of the earliest NPC components which starts to accumulate around chromosomes (Dultz et al., 2008) was used as a marker firstly. In a time point when GFP3-Nup153 first started to accumulate around chromosomes, a cell with GFP3-Nup153 expression was fixed with GA and prepared for TEM. In this cell, first attachment of ER sheets to non-core region of chromosomes have been observed clearly (Fig. 12). By being consistent with Nup153 accumulation around chromosomes, NPC-like structures have also been observed on the membranes attached to chromosome surface (Fig.12D, check red arrow on Fig.12D'). The membranes attached to chromosome surface on non-core regions also had unattached elongations with lots of fenestrations in both chromosome attached and unattached sides (Fig.12D, check empty arrows on Fig.12D'). Similar results have been obtained by using other NPC and NE markers like; BAF, LBR, Nup107 and Nup133.

NE and NPC assembly occurs in a later stage for the core region (core region is defined as a region of telophase chromosome mass with mitotic spindle attachment) of chromosomes (Haraguchi et al, 2001). Because of this reason a telophase cell has also been prepared with GFP3-Nup153 expression to relate the NPC formation on non-core region with core region. Comparable with the non-core region results, on the core region of chromosomes for early

telophase cells, NPC accumulation on the chromosome attached membranes and fenestrations on unattached elongations have also been observed (filled red arrows are NPC, empty arrow are fenestrations on Fig. 13).

These results prove that the fenestrated ER-sheets are the NE-precursors and they form the NE by starting from non-core region. The early existence of NPC-like structures on chromosome attached regions of membranes is also a proof for the use of fenestrations for post-mitotic NPC assembly. The NE formation start from non-core regions with ER sheets have been reported previously by both fluorescence and electron microscopy techniques with no report of high abundance of fenestrations (Lu et al., 2011; Fichtman et al., 2010; Macaulay and Forbes 1996). However, a recent report made according to cryo-EM imaging mentions the existence of these fenestrations on anaphase cells and refers their importance on NPC formation (Otsuka et al, 2018).

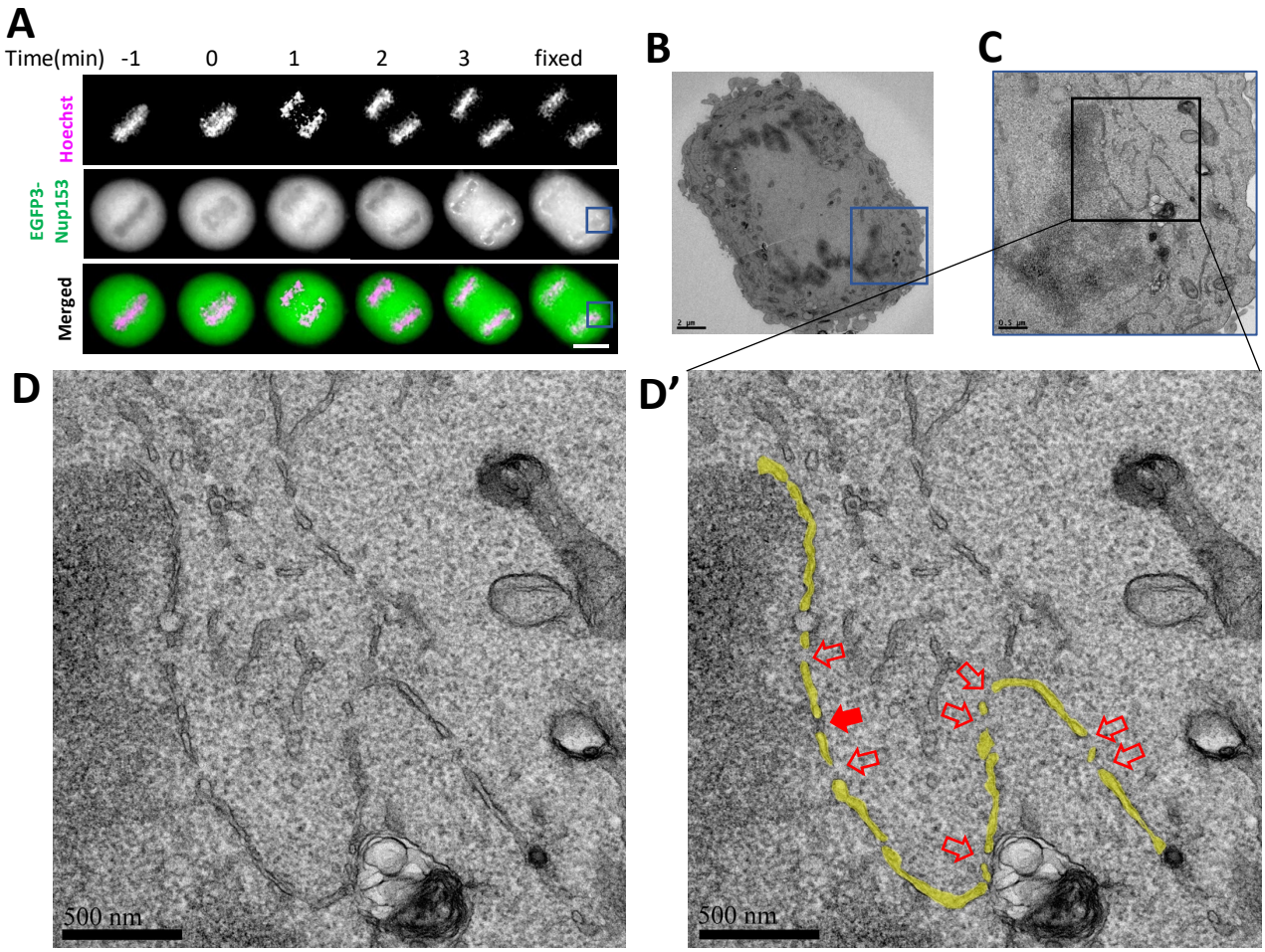

Figure 12. Chromosome attached regions of ER sheets start to have NPC-like structures in early telophase cells. (A) Time-lapse image of the fixed cell with EGFP3-Nup153 expression. Scale bar is 10 μm. (B) Low magnification EM image of the same cell. (C) high magnification image of blue square on B. (D) Enlarged black region on C. (D') Same image on D is colored for membranes on yellow. NPC-like structure is shown with red arrow. Fenestrations are indicated with empty arrows.

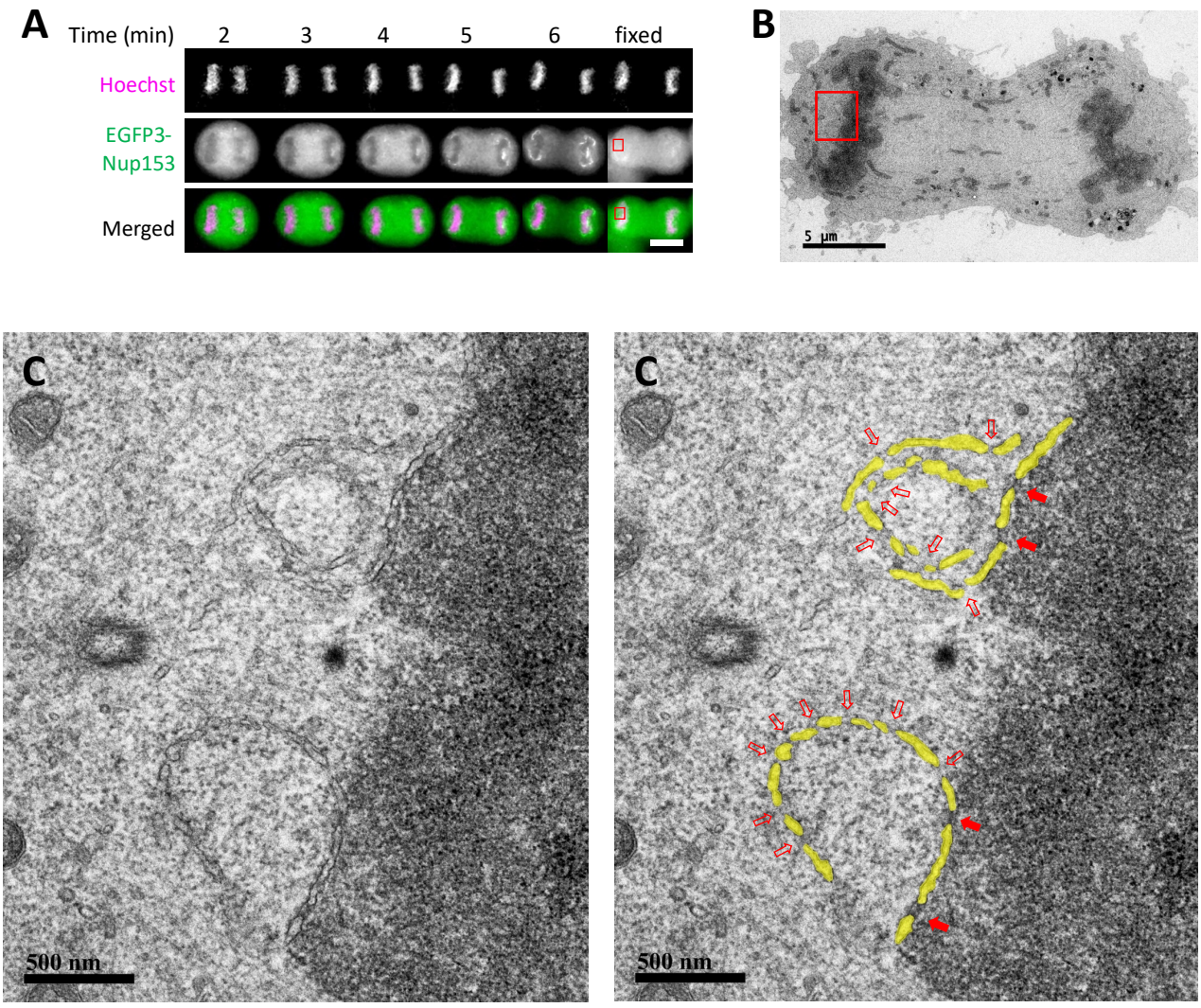

Figure 13. Core region of chromosome also shows similar NPC-like structure accumulation on chromosome attached membranes while showing mostly empty looking holes (fenestrations) on unattached region. (A) Time-lapse image of the fixed cell with EGFP3-Nup153 expression. Scale bar is 10 µm. (B) Low magnification EM image of the same cell. (C) High magnification EM image of the red square on B. (C') Membranes are superimposed on yellow for the same image on C. NPC-like structures are shown in Red arrows. Fenestrations are shown with empty arrows.

First collected NPC components around chromosomes

To confirm that Y-complex components and also Nup153 starts to be collected around chromosomes earlier than NE transmembrane proteins, cell with EGFP tagged nucleoporins and NE proteins were observed time-lapse. From several samples for each component fluorescence intensities are measured for chromosomes and nuclear rim areas. Measured

intensities were normalized, averaged and the graph on fig. 6C has been obtained. As seen from the graphs and compared fluorescence images, Y-complex components Nup107 and Nup133 collects around chromosomes earliest and Nup153 follows it (Fig. 14). This result is consistent with previous reports (Bodoor et al., 1999; Daigle et al., 2001; Belgareh et al., 2001; Dultz et al., 2008).

Nup133 and Nup153 can collect NE-like and NPC-like structures without DNA interaction

As shown in the previous section, Nup133 and Nup153 are nucleoporins reported previously for their early accumulation around chromosomes before than other nucleoporins and also transmembrane NE proteins like LBR. This early accumulation of these proteins may be important for post-mitotic NPC assembly. As an addition to this, Nup153 and Nup133 are claimed to have direct interaction with NE (Vollmer et al., 2015; Doucet et al.,2010) which may also be important for the first NE interaction of NPCs at the end of mitosis. Also, Y-complex components (includes Nup133) are essential for NPC formation because when they are depleted from Xenopus egg extracts, intact membranes without NPC forms around chromosomes (Harel et al., 2003; Walther et al., 2003; Boehmer et al., 2003a). Because of these reasons Nup133 and Nup153 were used as an effector molecule to see their NPC formation abilities.

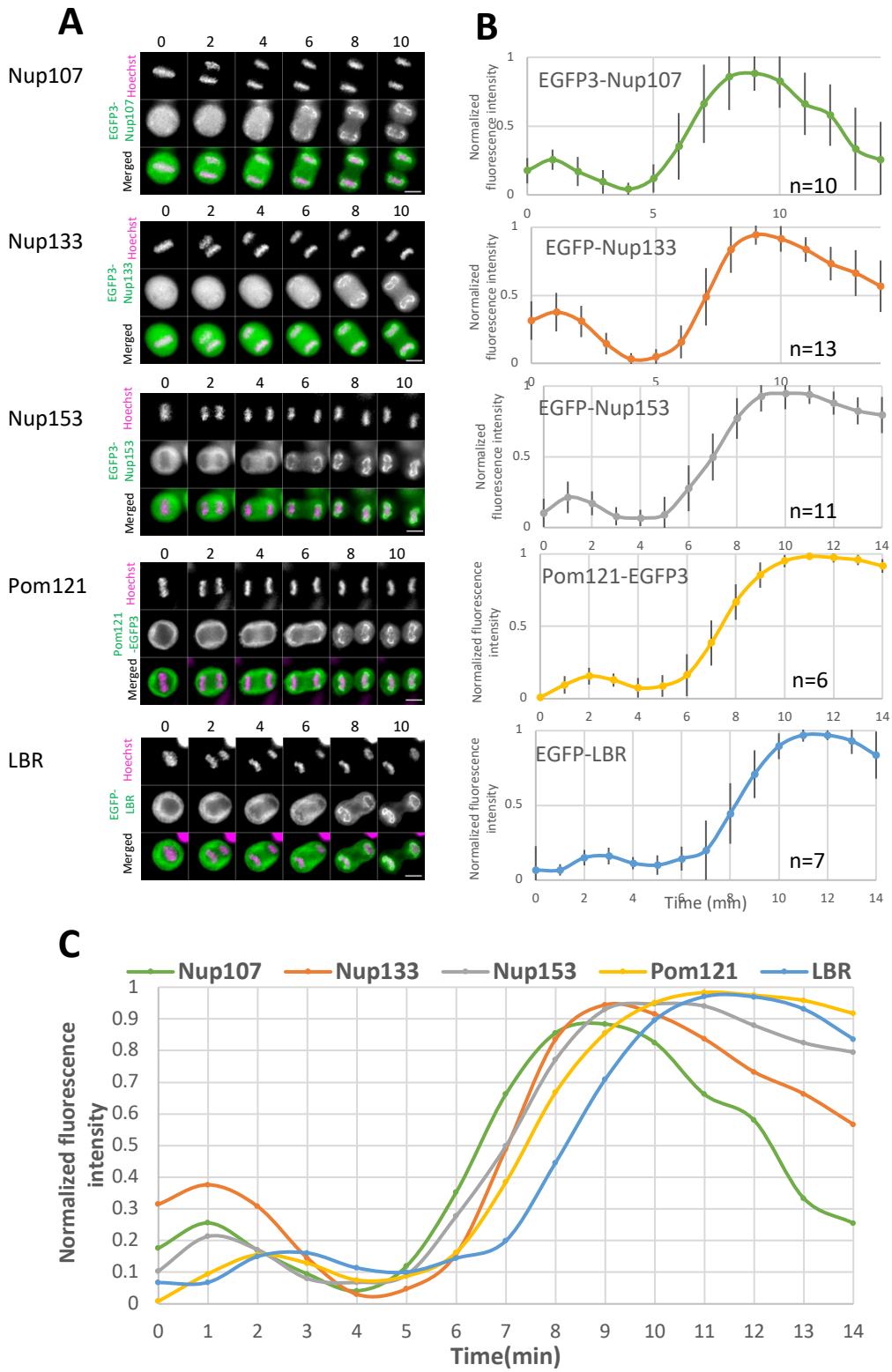

Figure 14. Accumulation times of nucleoporins around chromosome mass after anaphase onset. (A) Representative fluorescence images for each component. Numbers are showing the time points after anaphase onset in minute. (B) Averaged fluorescence intensities around chromosome and nuclear rim area for each component. Error bars are SD. (C) Merged graphs to compare first accumulation times of components around chromosomes.

To investigate the abilities of Nup133 and Nup153 in NPC formation, GFP antibody conjugated beads were inserted inside of EGFP-Nup133 stably expressing and also EGFP-Nup153 stably expressing HeLa cells. After one day incubation, cells with GFP positive bead inside have been observed live and fixed in 1 h after anaphase onset. NE-like double layered membranes and also NPC-like protein dense structures are formed around the beads according to EM images (Fig. 15). (Beads with EGFP-Nup133 and EGFP-Nup153 coat will be mentioned as Nup133-bead and Nup153-bead respectively on following parts of this report.) This specific formation can be related to the existence of EGFP-Nup133 and EGFP-Nup153 around the beads because single layer membrane related to degradation system (lysosome) forms around negative control beads (Fig. 16). As negative control, anti-GFP beads were inserted inside of only GFP expressing HeLa cells and the similar live-CLEM experiments were repeated. To see the native NE and NPC structures, images of native nucleus on Fig.17 can be compared to the NE-like and NPC-like structures around the beads on Fig. 15.

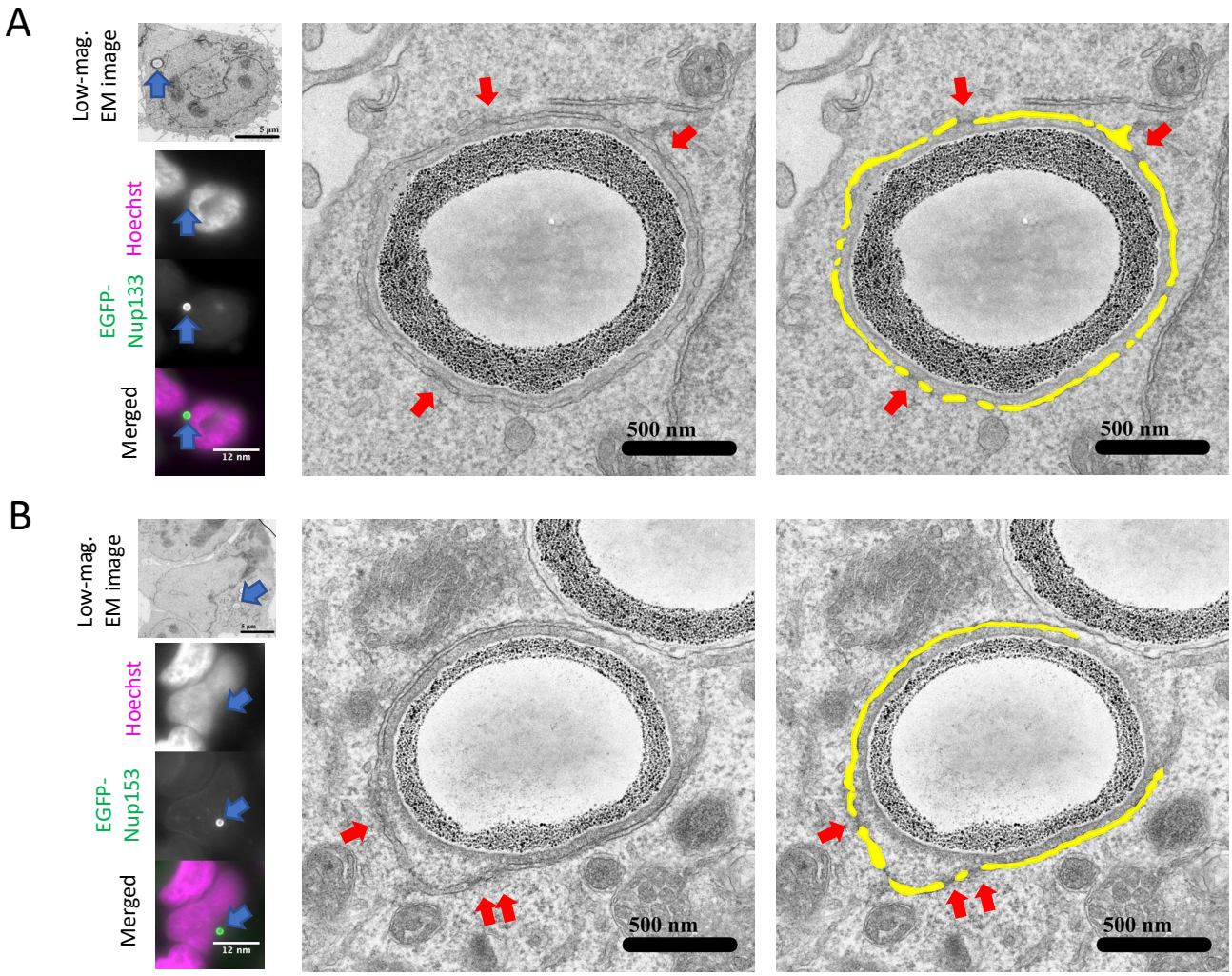

Figure 15. EGFP-Nup133 and EGFP-Nup153 coated beads can collect NE-like and NPC-like structures around. (A) The fluorescence and low magnification TEM images of an interphase cell with an EGFP-Nup133 positive bead (blue arrows) in the left and the high magnification image of the bead in the middle. On the right, the same image in the middle is colored for double layered membranes in yellow. NPC-like structures are shown with red arrows. (B) The fluorescence and low magnification TEM images of an interphase cell with an EGFP-Nup153 positive bead (blue arrows) in the left and the high magnification image of the bead in the middle. On the right, the same image in the middle is colored for double layered membranes in yellow. NPC-like structures are shown with red arrows.

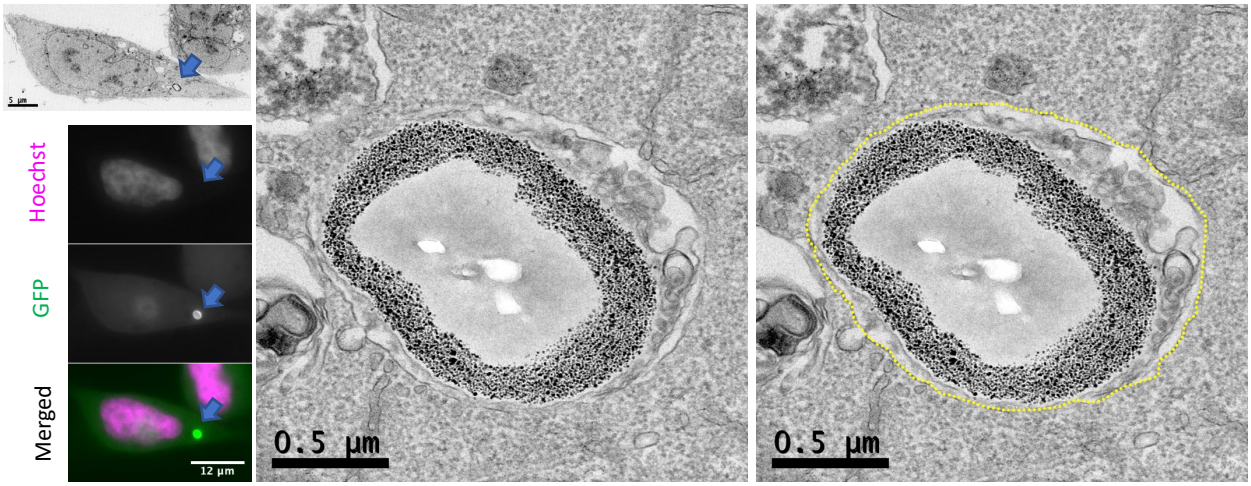

Figure 16. GFP conjugated beads are covered with single layered membrane. On the left side, low magnification EM image and also fluorescence images of the same GFP expressing cell can be seen. In the middle, high magnification image of the bead indicated with blue arrows on the left side is shown. The yellow colored single layered membrane around the bead for the same image can be seen on the right side. Blue arrows are showing the GFP covered bead.

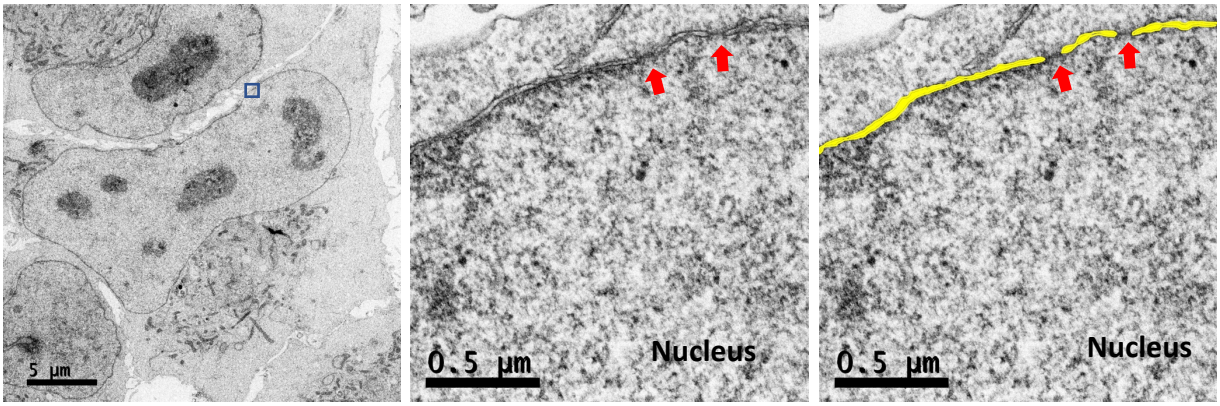

Figure 17. An example views of NPC and NE on nucleus. The blue square on the left low magnification image is enlarged in the middle and the right images. Red arrows are indicating the NPCs. On the right, the same image in the middle is colored for NE in yellow.

Nup133 and Nup153 collect different nucleoporins

After anti-GFP bead insertion, cells were incubated 1 day in CO_2 incubator. The reason for this incubation was to increase the number of cells inside the dish with a GFP-positive signal which have at least one mitosis, because the duration of HeLa cell cycle is around 24 h. After 1-day incubation, cells were fixed and treated with antibodies against other nucleoporins. According to this immunofluorescence staining results, it has been seen that Nup133-beads can collect mostly the intra-complex components Nup107 and ELYS while it cannot collect mAb414 antibody efficiently which recognizes the FG-repeats on nucleoporins (Fig. 18A, B and C). Interestingly this beads also have been seen not to interact with Pom121 (Fig.18D) being a transmembrane nucleoporin and reported as interacting with Y-complex (Mitchell et al., 2010; Schwartz et al., 2015). The reason for this difference between previous data and current data may be the absence of DNA around the beads, because Nup133 has been reported to collect Pom121 according to observations of LacI/LacO system which includes the interaction of DNA (Schwartz et al., 2015). On the other hand, as being different from the Nup133, Nup153 cannot collect Y-complex components Nup107 and ELYS around beads (Fig. 18A and B). Also, Nup153-beads were mostly positive for mAb414 antibody (Fig. 18C), which is probably because of the FG-repeat exists on Nup153. However, for other FG-repeat including nucleoporins (Nup98, Nup62 and Pom121), Nup153 showed a more efficient level of collection around the beads compared to Nup133 (Fig. 19). Nup153 can also collect Pom121 efficiently (Fig. 18D). Pom121 also includes FG-repeat. FG-repeat on Nup153 may be the main reason to collect other FG-repeat including nucleoporins and FG-Nups may have an affinity for each other. Some nucleoporin antibodies were used in similar ways and the number of GFP positive beads together with antibody positive beads were counted for 3 different dishes and the numbers were normalized to a total of 100 GFP positive beads and averaged. Averaged values were graphed by using standard deviations as error bars (Fig. 19).

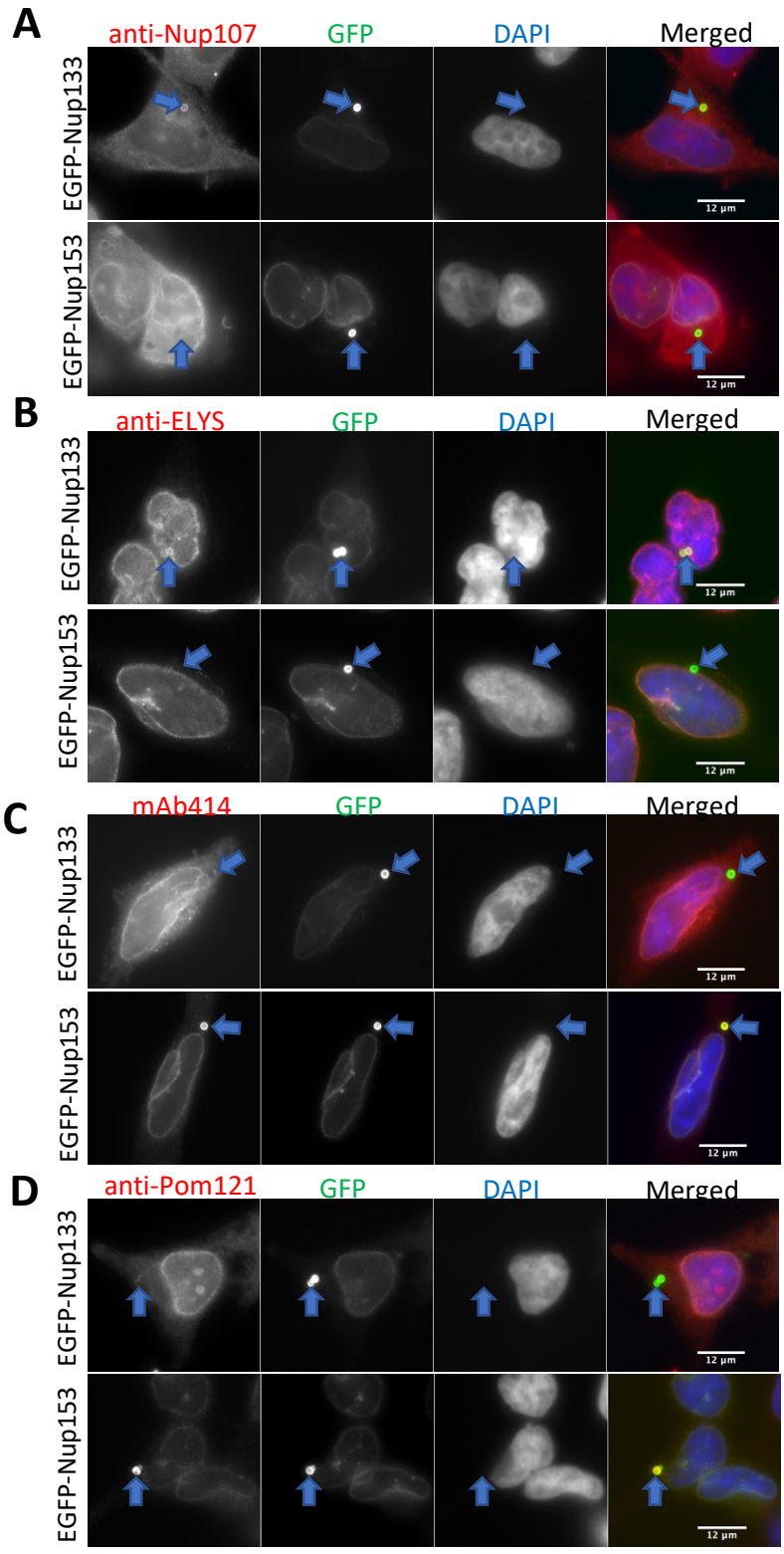

Figure 18. EGFP-Nup133 and EGFP-Nup153 collects different nucleoporins. (A) Representative images for Nup107 accumulation around Nup133 and Nup153-beads. (B) ELYS accumulation around Nup133 and Nup153-beads. (C) mAb414 signal around Nup133 and Nup153-beads. (D) Pom121 accumulation around Nup133 and Nup153-beads.

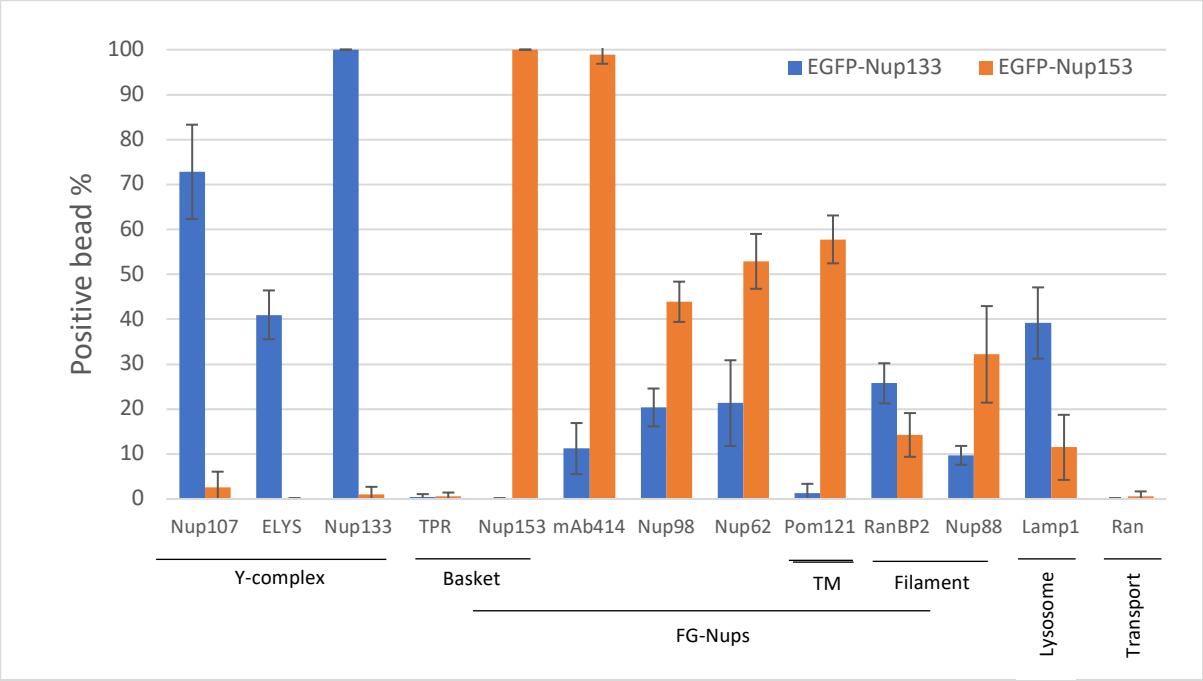

Figure 19. Compared antibody collecting abilities of Nup133 and Nup153.

NE-like structures and NPC-like structures form around the EGFP-Nup133 and EGFP-Nup153 beads inside telophase cells too

In the same way with previous experiments, anti-GFP beads were inserted inside of HeLa cells which have stable EGFP-Nup133 or EGFP-Np153 expressions. After 1-day incubation, cells with a GFP-signal positive bead were used for live observation. In 15th min after anaphase onset, cells were fixed, and the same cell prepared for TEM. NPC or NE formation around the beads were observed. For both molecules EGFP-Nup133 and EGFP-Nup153, in 15th min after anaphase onset, NE-like and NPC-like structures accumulated around the beads (see Fig. 20 for Nup133 and Fig. 21 for Nup153) similar to interphase cells, which means both NPC components capable of forming NPC-like structures post-mitotically. As an addition to these NE-like and NPC-like structures, some number of fenestrations are also observed on the double layered membrane around the beads (empty arrows on Fig.20C' and Fig.21C', circles on the top views of the beads on Fig.20D' and Fig.21D').

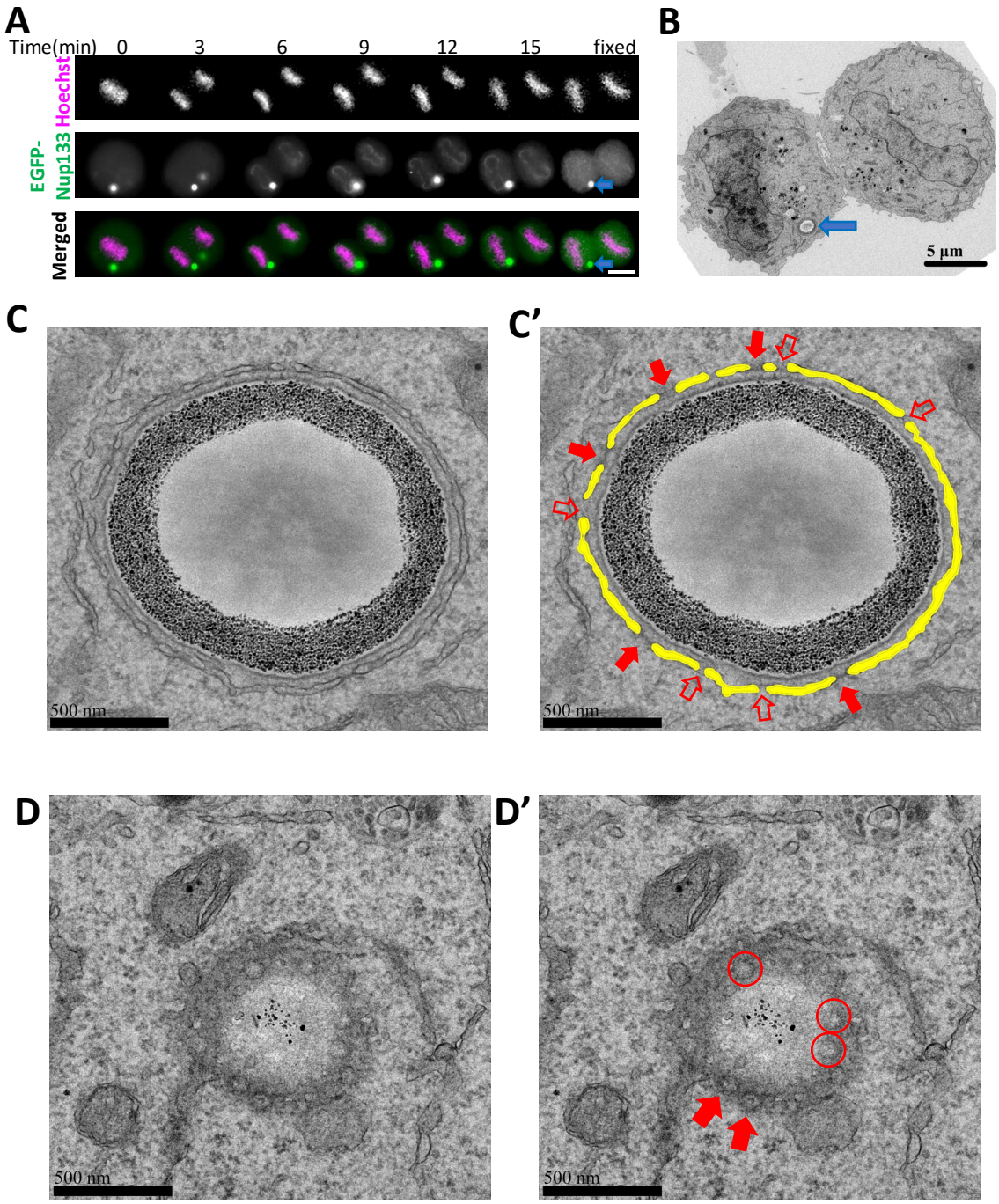

Figure 20. NPC-like structures and NE-like structures are collected around EGFP-Nup133 conjugated beads during telophase. (A) Time-lapse fluorescence image of the cell with fixed time point. Target bead is shown with blue arrow. Scale bar is 10 µm. (B) Low magnification TEM image of the fixed cell. Target bead is indicated with blue arrow. (C) High magnification image of the target bead. (C') Same image on C is colored with yellow for double layered membranes. NPC-like structures are shown with red arrows. Fenestrations are shown with empty red arrows. (D) Top view of the target bead. (D') Fenestrations (red circles) and NPC-like structures (red arrows) are indicated for the same image on D.

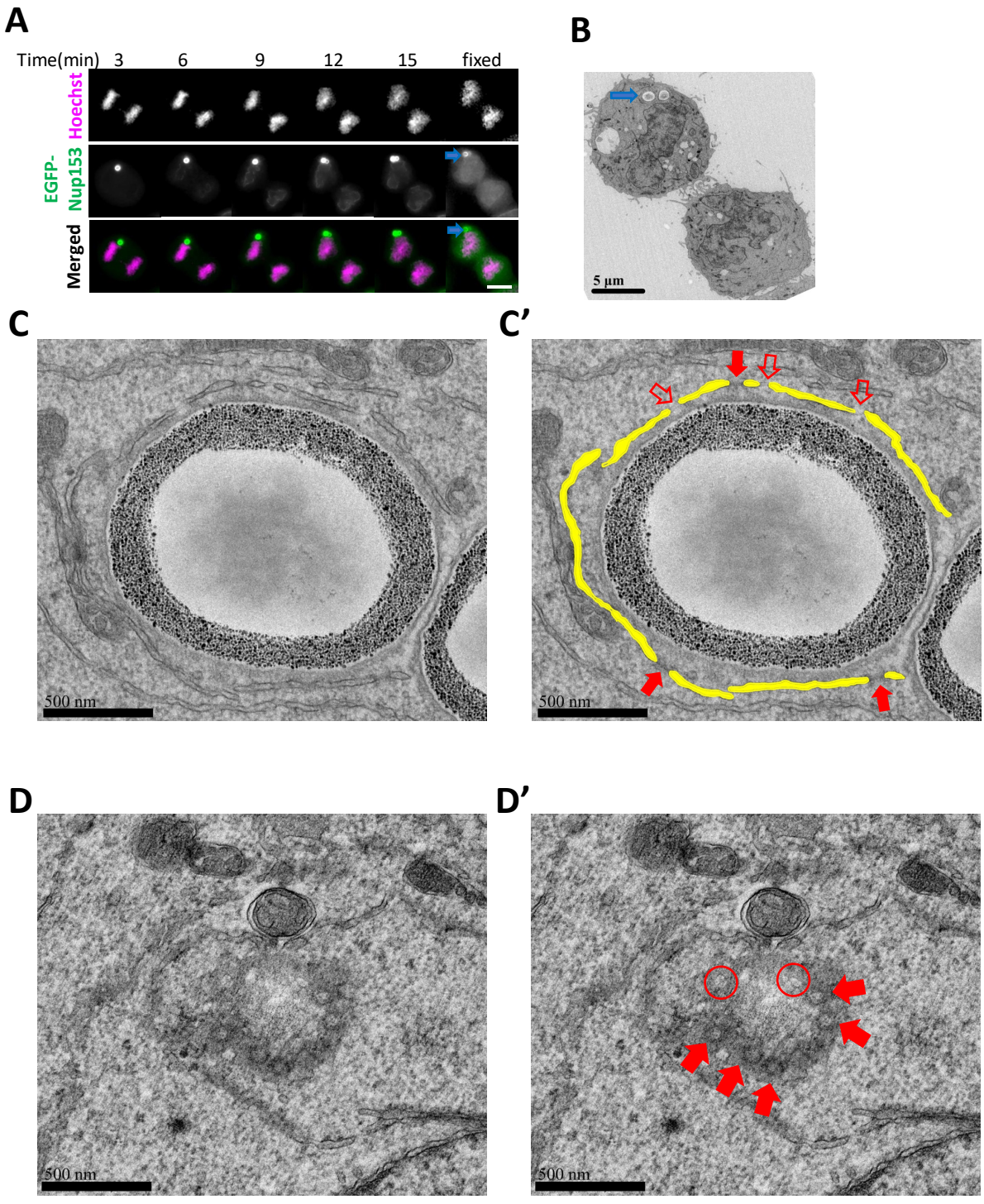

Figure 21. NPC-like structures and NE-like structures are collected around EGFP-Nup153 conjugated beads during telophase. (A) Time-lapse fluorescence image of the cell with fixed time point. Target bead is shown with blue arrow. Scale bar is 10 µm. (B) Low magnification TEM image of the fixed cell. Target bead is indicated with blue arrow. (C) High magnification image of the target bead. (C') Same image on C is colored with yellow for double layered membranes. NPC-like structures are shown with red arrows. Fenestrations are shown with empty red arrows. (D) Top view of the target bead. (D') Fenestrations (red circles) and NPC-like structures (red arrows) are indicated for the same image on D.

Nup133 and Nup153 has different affinities for membranes on post-mitosis and metaphase

A difference has been observed on EGFP-Nup133 and EGFP-Nup153 positive beads inside telophase cells (15th min after anaphase onset) for the distance of the membranes to the bead surface. The membranes around Nup133-beads appeared to be closer to the bead surface than those around Nup153-beads (compare yellow shading in Figs. 20C′ and 21C′). As described in methods section, the distance of membranes to the surface of the beads have been quantified for 3 samples for each Nup133 and Nup153 covered beads. And the graphs on fig. 14 have been prepared. The mean distance calculated from three different beads was 33.1 ± 5.5 nm (mean ± standard deviation (SD)) for Nup133-beads and 72.9 ± 3.4 nm (mean ± SD) for Nup153-beads (Fig. 22A). As an addition to this difference, Nup133-beads exhibited a more uniform coverage for membranes than 153-beads. To show this, instead of averaging the averaged distances from 3 samples, all measured distances have been used and a higher SD amount have been seen on Nup153-beads; Nup133-beads (32.6 ± 11.7 nm, mean ± SD, total of 407 measurements in three beads) Nup153-beads (73.1 ± 30.7 nm for total 335 measurements in three beads).

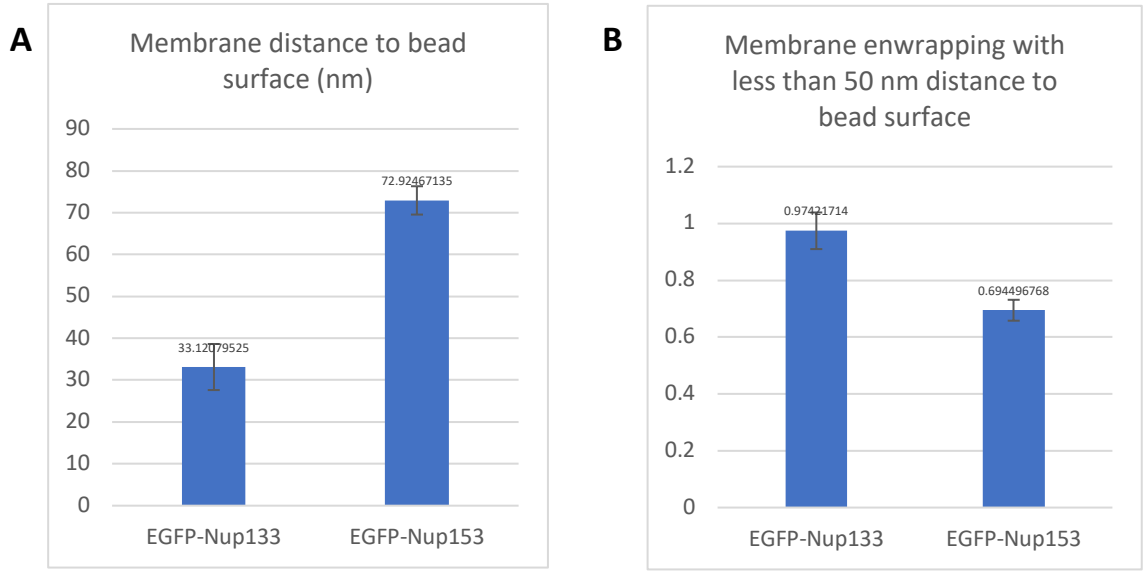

Figure 22. Membrane relation of Nup133 and Nup153 on post mitosis. (A) The graph showing the membrane distance to bead surface for each Nup133 and Nup153-beads. (B) The graph showing the ratio membrane length to bead surface length.

Because of this nonuniform coverage around Nup153-beads, the membranes closer to the bead surface than 50 nm has been decided to have direct relation with the components around the beads. The reason for this decision was the predicted length of streptavidin-biotin complex GFP antibody and also the GFP protein around the beads were at most ~45-50 nm. According to this decision, less interaction of membranes to the bead surface has been observed on Nup153-beads than Nup133-beads (Fig. 22B).

To confirm this membranal efficiency of Nup133, I also used beads for metaphase cells. Similar to telophase cells, Nup133-beads exhibited a high affinity for membranes than Nup153-beads during metaphase (compare yellow shades around the beads on Fig.23A and B). The membranes around Nup133-beads were tightly packing the membrane while they were looser on Nup153-beads. This result also has been quantified by using 3 beads for each and similar results with telophase cells obtained (check Fig. 23C). The average distance of membranes to Nup133-bead surface was 32 ± 8.09 (mean ±SD) while it was 77.04 ± 20.2 for Nup153-bead.

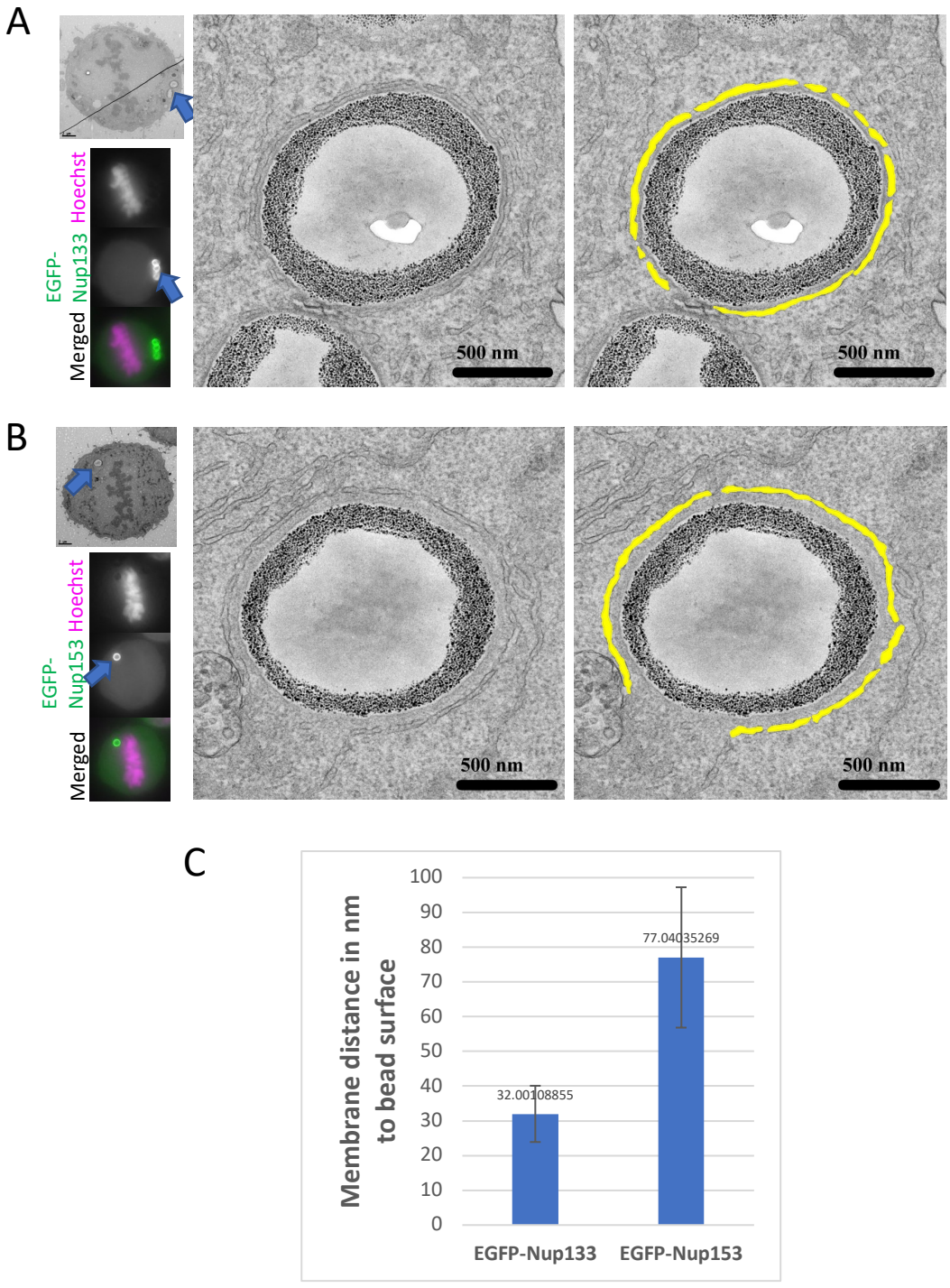

Figure 23. EGFP-Nup133 and EGFP-Nup153 coated beads have different affinities for membranes during metaphase. (A) A CLEM sample for Nup133-bead with fluorescence and low magnification images on the left, high magnification image on the middle and yellow drawings for membranes are superimposed on the right side for the same image in the middle. (B) A CLEM sample for Nup153-bead with fluorescence and low magnification images on the left, high magnification image on the middle and yellow drawings for membranes are superimposed on the right side for the same image in the middle. (C) Quantified distances of membranes to bead surface for 3 samples for each Nup133 and Nup153 beads.

The structure of membranes collected around Nup133 and Nup153 are different on fenestration number for telophase cells

Another difference on the membranes collected around Nup133 and Nup153 beads was the structure of the membranes. As seen from the top and side views of the beads (Fig. 20 and 21, shown with empty arrows on side and circles on top views), both Nup133 and Nup153 includes, together with NPC-like structures, the empty looking fenestrations on membranes. The number of empty looking fenestrations was quantified from 3 different samples for each Nup133 and Nup153, for the membranes in 50 nm or less distance to bead surface (which is considered as the direct relation of membranes to bead component). The number of fenestrations per 10 µm membrane around Nup153-beads were significantly less than Nup133-beads (Fig. 24). It means that Nup133 can collect more fenestration including membranes or it can create the fenestrations itself. Both may be true when the structural feature of Nup133 has been considered. For further explanation and possibilities please see the discussion part.

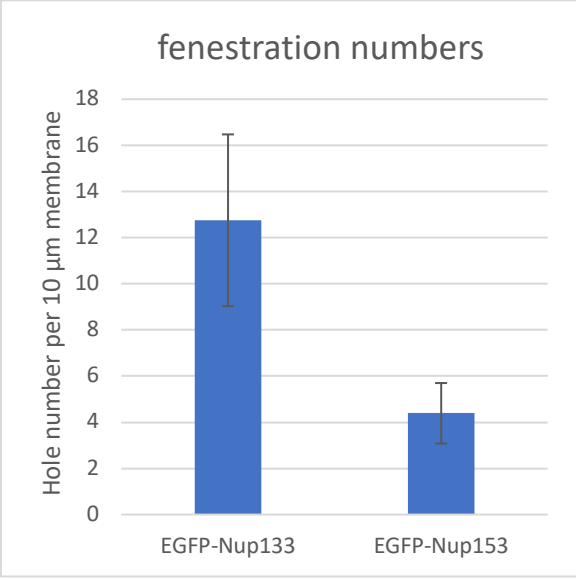

Figure 24. Compared fenestration amounts around the membranes for Nup133 and Nup153 beads

Membrane curvature affects the NPC formation post-mitotically

Different size beads have been inserted inside of the cells; 3 μm and 1.6 μm in diameter (will be mentioned as 3 μm-bead and 1.6 μm-bead afterwards). In similar way with previous experiments, cells have been started to be observed live after 1-day incubation and fixed with GA on 15th min after anaphase onset. In this time point, similar to interphase cells, beads collect some NPC-like and also NE-like structures. The number of NPC-like structures around NE, 3 μm-bead and 1.6 μm-bead has been counted as described in methods section (red arrows in Fig. 25 A-F). Counted results have been graphed in comparison with each other for both EGFP-Nup133 and EGFP-Nup153 expressing cells. As seen from the figure 25G, the number of NPC-like structures per 10 μm membrane changes significantly between 3 μm and 1.6 μm-beads for both nucleoporins. 1.6 μm-beads which has a high degree of membrane curvature than native NE and 3 μm-bead, collect more NPC-like structures. Both size beads also have more amount of NPC-like structures than the native NE, which is probably related again to the curvature degree of the membranes. This result clearly shows the effect of curved membranes on NPC-formation post-mitotically.

As an addition, 3μm-beads covered with Nup133 has more NPC compared to the same size Nup153 covered beads. The number of NPC-like structures on the 1.6-μm beads and the 3-μm beads for Nup153 was 7.5 ± 1.0 and 2.6 ± 0.1 respectively (mean ± SD for three different beads). On the other hand, these numbers for Nup133 was 8.1 ± 0.9 for 1.6-μm beads and 4.7 ± 1.1 for 3-μm beads (mean ± SD for three different beads). As seen from these numbers, when the bead size is larger, NPC amount formed around the beads for Nup153 has sharper decrease than Nup133 (compare the differences on NPC number for different size beads for each nucleoporin). It means that membrane curvature effect is less on Nup133 compared to Nup153. The reason for this change may be because of the so claimed role of Nup133 on forming or recognizing high curvature membranes, the fenestrations.

These results suggest that both Nup133 and Nup153 collect the NPC or its intermediates more efficiently on the membrane surface with a higher curvature on the reforming membranes in an early stage of NE reformation.

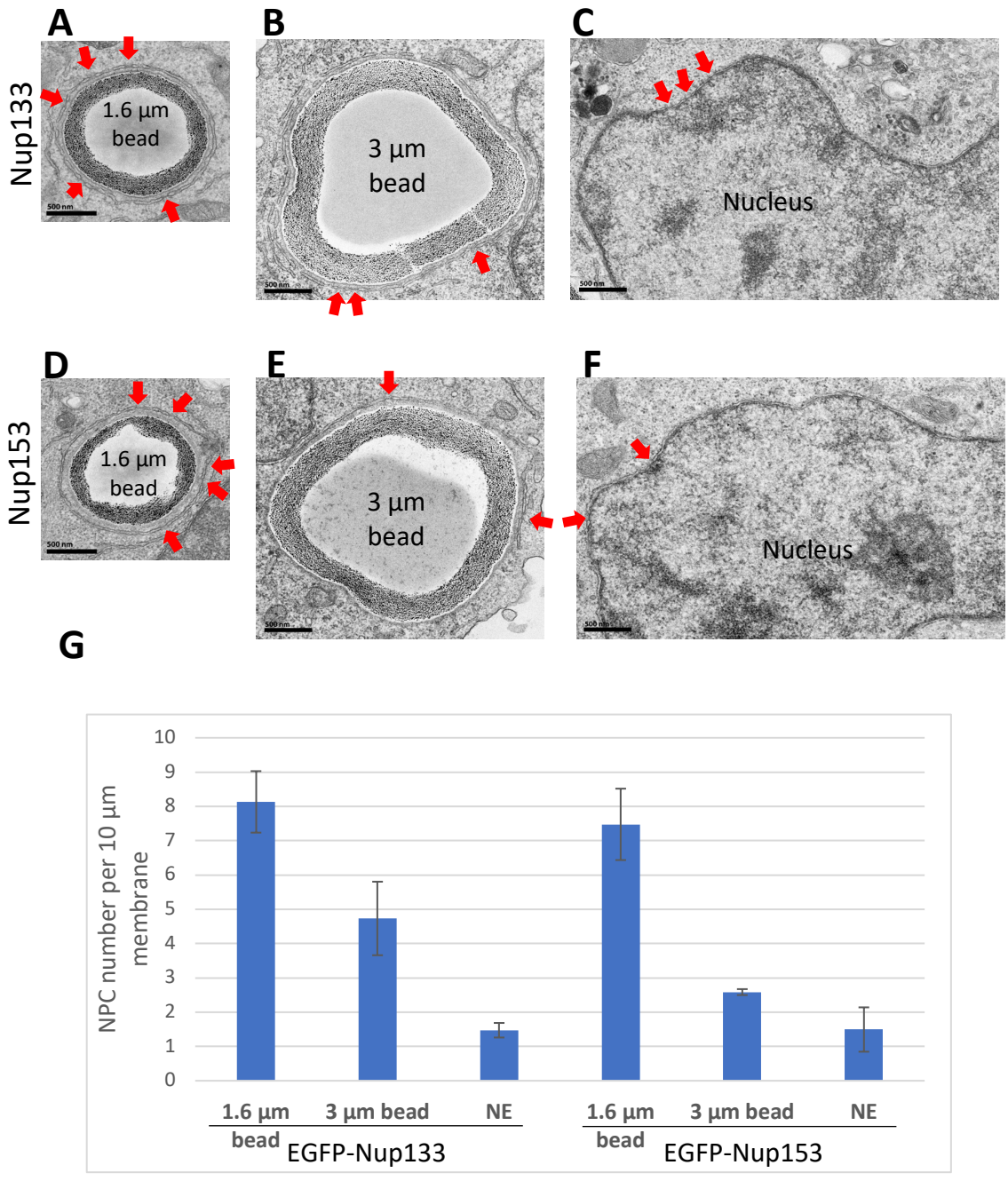

Figure 25. The effect of membrane curvature on NPC formation at the end of mitosis. The NPC or NPC-like structures area indicated with red arrows in different size beads and also in nucleus for EGPF-Nup133 expressing (A, B, C) and EGFP-Nup153 expressing (D,E,F) cells. (G) Quantified NPC amount on different size beads and NE for three experiments. Error bars are standard deviations

Conclusion

In this research firstly the NE reformation is investigated. It has been clearly observed that NE starts to form from sheet-like fenestrated ER membranes (Figs. 8-11). The empty looking fenestrations on ER membranes of early dividing cells were observed to be filled on the chromosome attached parts on the later stages of cell division (Figs. 12-13).

As a second step, post-mitotic NPC assembly mechanisms related to fenestration recognition are tried to be investigated. Nup133 and Nup153 are the earliest accumulating components of NPC around chromosomes after anaphase onset (Fig. 14; Dultz et al., 2008). The single roles of these nucleoporins on NPC assembly was discovered by the help of bead-insertion technique. It has been shown for the first time that, Nup133 has an earlier affinity for double layered membranes which indicates a role for the first membranal interaction of NPC on post-mitotic assembly for this nucleoporin (Fig. 20-23). On the other hand, neither Nup133 nor Nup153 can collect all components of NPC which means none of them are the single starters of full NPC (Fig. 19). Compared to Nup153, Nup133 collects a greater number of fenestrations on double layered membranes (Fig. 24). And the early existence of fenestrated ER sheets on anaphase cells have been also observed (Fig.10-11). This expands the role of Nup133 for post-mitotic NPC assembly. Possibly, early accumulating Nup133 around chromosomes, interacts with double layer membranes through the fenestrations which already exists on the ER membranes. These results emphasize the importance of fenestrations on NE precursors for post-mitotic NPC formation. To support this idea, the effect of membrane curvature to NPC formation have been also examined (Fig. 25). Small size (1.6 μm in diameter) beads which have a higher degree of curved surface, collected higher amount of NPC-like structures compared to bigger size (3 μm in diameter) beads (Fig. 25G). Overall, instead of a so-claimed

single precursor model for NPC formation, multiple factors are working together to create full NPC at the end of mitosis.

As a conclusion for all results, I propose a new model here (Fig. 26). According to this model, fenestrations exist in high amount on mitotic ER membranes which will be the precursors of NE. These fenestrations are recognized by Nup133 including Y-complex components possibly by directly anchoring the membrane. After the attachment of Nup153, other components of NPC are collected on the fenestration and the full NPC is formed.

Also, it is important to mention that, as being a novel method used in this research, bead insertion technique is a promising approach to search the roles of proteins inside living cells.

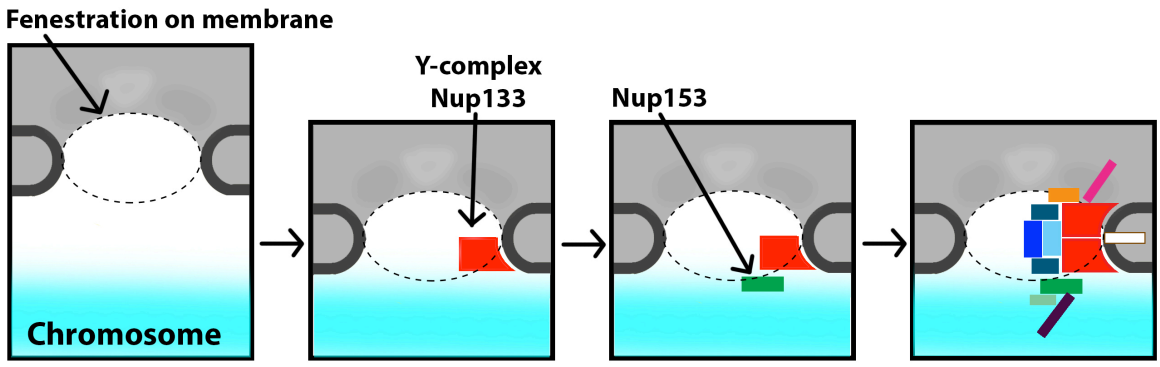

Figure 26. A new model proposed for NPC formation at the end of mitosis.

Discussion

Nucleoporin-nucleoporin interaction for NPC formation

Both EGFP-Nup153 and EGFP-Nup133 has the ability to form structures looking like NPC under EM. However, they collect different types of nucleoporins in different efficiencies. While Nup153 can collect FG-Nups and Pom121, it cannot collect observed Y-complex components Nup133, Nup107 and ELYS (Fig.19). Also, Nup133 can collect its own sub-complex components Nup107 and ELYS but collects FG-Nups less efficiently than Nup153. Nup133 also cannot collect Nup153 and Pom121 which is a transmembrane nucleoporin. According to previously made Lac-I/Lac-O experiments, Nup133 and Nup153 was observed to collect most components of NPC (Schwartz et al, 2015). As being different from my results, in these experiments both Nup133 and Nup153 were shown to collect Pom121 nucleoporin (Schwartz et al, 2015). Also, for Nup153, an average level of Y-complex component accumulation has been observed (Schwartz et al. 2015). The reason for these uncorrelated observations can be the effect of chromosomes, since the Lac-I/Lac-O system resides inside the nucleus. Nup153 is also reported as it can interact with membranes with its N-terminal domain previously (Vollmer et al, 2015). With the help of its interactions with membranes, Nup153 is thought to recruit Y-complex components to NE in interphasic cells (Vollmer et al, 2015). Interestingly DNA conjugated beads couldn't collect any NPC-like structures (Kobayashi et al., 2015). However, according to in-vitro experiments done previously, instead of naked DNA strand, nucleosomal chromatins are presented as necessary for NPC recruitment (Zierhut et al. 2014). Overall, these results suggest that Nup133 or Nup153 cannot collect full NPC with the absence of nucleosomal chromatins. These all suggests that, possibly, instead of a one seed starter for NPC, there is a complex order which includes nucleoporins, membranes, DNA and histone proteins all together. To clarify the role of each nucleoporin on NPC

assembly, similar experiments have to be done further for all nucleoporins to understand the NPC assembly overall.

As an addition to these, NPC assembly regulators should also be kept in mind. It is known that nucleoporins have to be phosphorylated to be released from NE at the onset of mitosis (for review Worman and Courvalin, 200; Burke and Ellenberg, 2002). Inversely, at the end of mitosis they have to be dephosphorylated to be collected on NE (for review Champion et al, 2017; Schellhaus et al., 2015). Cell cycle dependent kinases and phosphatases are thought as the major regulator for this phosphorylation and dephosphorylation process on entrance and exit of mitosis. As an addition to these regulators, Ran and other transport receptors are thought as regulators for NPC assembly during interphase and mitosis too (D'Angelo et al., 2006; Walther et al., 2003). By using bead insertion method further analysis done with these regulators may help to elucidate the regulation mechanisms of NPC assembly.

It should also be noted that Lamp1 which is a lysosomal transmembrane protein was observed to be collected around Nup133 and Nup153 beads in ~40% and ~15% amount respectively (Fig. 19). It means that some beads for both components are targeted by autophagy and thrown away to lysosome. In other words, it can be said that Nup153 can escape autophagy more efficiently than Nup133. By comparing the accumulation averages for Nup107 and Lamp1, it can be said that some fraction of Nup133-beads which has interacted with Nup107 are still targeted by autophagy. This less efficiency of Nup133 to escape from autophagy is intriguing and also difficult to interpret.

Importance of membranal structures on NPC formation

NPC formation is defined to happen in two different mechanisms for metazoans; during interphase and at the end of mitosis. Multiple differences in these two types of NPC formation has been reported before. These differences include sequential addition of nucleoporins and

also the total formation time. At the end of mitosis NPC forms around 10 min (Dultz et al., 2008), while it takes more than 30 min for an interphase NPC to form (Dultz et al., 2010). The slow NPC accumulation is generally related to the NPC formation on intact double layer membrane during interphase. Being different from this, at the end of mitosis NPC forms together with NE, and in theory it effects the formation time of NPC. However, there are several reports for the formation of NE whether it forms from tubular ER (Anderson and Hetzer, 2007) or sheet-like intact ER (Lu et al., 2011). In the case of an intact sheet-like NE formation, post-mitotic NPC formation won't have a clear difference on formation from interphase. It is strongly accepted that the NE starts to form from non-core regions of the chromosomes (Haraguchi et al., 2001) which is also consistent with the data I obtained in this research. It is possible to think that with enclosure model, intact membranes attached to non-core region can extend and cover the pre-existing pre-pores on core regions on chromosome surface and creates the first NPCs on post-mitosis. However, it is also strongly being accepted that core region of chromosomes are the main regions of pore-free islands which lacks NPC just after mitosis (Maeshima et al., 2006; Vietri et al., 2015) and the NPC in this region mostly forms during interphase (Otsuka et al., 2016). This means that if NE forms from intact ER sheets, NPCs will form in the same way as interphase and it should take the same time but the quick assembly of NPCs at the end of mitosis reported by several groups (Dultz et al., 2008; Haraguchi et al., 2000; Lu et al., 2011). As shown in my research, instead of an intact ER sheet, NE starts to form from fenestrated ER sheet (Figs 8-11). The fenestrations residing on the NE precursors are good candidates to position the newly forming NPCs and enable a quick formation.

One of the possible nominees to recognize these fenestrations on NE precursors is Nup133, because it accumulates around chromones earlier than other nucleoporins (Fig. 14) and also it has a structure similar to vesicle coating proteins (Devos et al., 2004; Bigay et al., 2005; Grin et al., 2007). My results from this project support this idea because of early affinity of Nup133 for dense fenestrated double layer membranes (Fig. 24). Nup133 has a domain called as ALPS domain which is suggested to be imported for recognition of high curved structures (Grin et al., 2007; Doucet et al., 2010; Doucet et al., 2015). However, it has also been argued that ALPS domain may not be necessary for post-mitotic NPC formation while this domain was necessary for interphase NPC formation (Doucet et al, 2010). In this report from year 2010, only the nuclear rim targeting of wild type (wt) and ALPS-null mutants of Nup133 were being compared during anaphase and interphase. They saw that during anaphase both wt-Nup133 and ALPS-null Nup133 could be targeted to the chromosome surface in a similar manner, while ALPS-null mutant could not target the nuclear rim during interphase according to fluorescence imaging (Doucet et al., 2010). To find out which domain of Nup133 is important for early membrane affinity, further experiments with ALPS-null mutants are necessary with high resolution imaging techniques. Previously it was thought that first membranal interaction of NPC is done by Pom121 according to stepwise accumulation observation of NPC components on fluorescence microscopy (Dultz et al., 2008). However according to my results, Nup133 has a high affinity for double layered membranes during metaphase and also late telophase, which supports a new model for the formation of NPC post-mitotically. According to this new model, early accumulated Nup133 around non-core region of chromosomes interacts with the fenestrations on the membranes simultaneously, and Pom121 comes afterwards.

Nup153 is reported to have an amphipathic helix domain which helps it to recognize membranes (Vollmer et al., 2015; Mészáros, et al., 2015). Previously it has been shown that Nup153 interacts with interphase NE and an important starter for interphase NPC assembly

(Vollmer et al., 2015). Because Nup153 also starts to be collected around chromosomes earlier than most of the nucleoporins (Dultz et al., 2008; Fig. 1), I thought that it may also engage with membranes during mitosis too and may help NPC formation post-mitotically. However, it has been clearly shown here that the affinity of Nup153 to double layered membrane is much less than Nup133 (Fig. 20-23). Thus, the early accumulation of Nup153 around chromosomes during cell division is not because of its membranal interaction but may be because of its efficient ability to collect FG-Nups and Pom121 (Fig. 19). Since Nup133 cannot collect Pom121 and also less efficient to collect FG-Nups, it is so much possible that they have a role complementary with each other to form full NPC at the end of mitosis.

Finally, Nup133-beads and Nup153-beads induced NPC assembly. These results contrast those obtained using DNA-beads and BAF-beads, which induced formation of the NE-like membrane but not the NPC structure (Kobayashi et al., 2015). Importantly, in all of these cases, autophagy was avoided by NE formation. The beads, once exposed to the cytosol after endosomal breakdown, are attacked by autophagy unless they are protected by NE formation (Kobayashi et al., 2010; 2015). Therefore, this experimental system using the beads is a useful tool for studying the molecular basis of NE formation and NPC formation in living cells.

References

Maeshima K, Yahata K, Sasaki Y, Nakatomi R, Tachibana T, Hashikawa T, Imamoto F, Imamoto N. Cell- cycle-dependent dynamics of nuclear pores: pore-free islands and lamins. J Cell Sci 2006; 119: 4442– 51

Anderson DJ, Hetzer MW. Nuclear envelope formation by chromatin-mediated reorganization of the endoplasmic reticulum. Nat Cell Biol 2007; 9: 1160-66

Anderson DJ, Vargas JD, Hsuao JP, Hetzer MW. Recruitment of functionally distinct membrane e proteins to chromatin mediates nuclear envelope formation in vivo. J Cell Biol 2009; 186: 183-91

Ball JR, Ullman KS. Versatility at the nuclear pore complex: lessons learned from the nucleoporin Nup153. Chromosoma 2005; 114: 319–330

Bastos R, Lin A, Enarson M, Burke B. Targeting and Function in mRNA Export of Nuclear Pore Complex Protein Nup153. The Journal of Cell Biology 1996; 134: 1141-56

Bayliss R, Kent H, Corbett A, Stewart M. Crystallization and initial x-ray diffraction characterization of complexes of FxFG nucleoporin repeats with nuclear transport factors. J Struct Biol 2000; 131:240-7;

Belgareh N, Rabut G, Baï SW, van Overbeek M, Beaudouin J, Daigle N, Zatsepina OV, Pasteau F, Labas V, Fromont-Racine M, Ellenberg J, Doye V. An evolutionarily conserved NPC subcomplex, which redistributes in part to kinetochores in mammalian cells. The Journal of Cell Biology 2001; 154: 1147–60.

Berke IC, Boehmer T, Blobel G, Schwartz TU. Structural and functional analysis of Nup133 domains reveals modular building blocks of the nuclear pore complex. The Journal of Cell Biology 2004; 167: 591–97

Bigay J, Casella JF, Drin G, Mesmin B, Antonny B. ArfGAP1 responds to membrane curvature through the folding of a lipid packing sensor motif. The EMBO Journal 2005; 24: 2244–53

Bione S, Maestrini E, Rivella S, Mancini M, Regis S, Romeo G, Toniolo D. Identification of a novel X-linked gene responsible for Emery-Dreifuss muscular dystrophy. Nat Genet 1994; 8: 323–27

Bodoor K, Shaikh S, Salina D, Raharjo WH, Bastos R, Lohka M, Burke B. Sequential recruitment of NPC proteins to the nuclear periphery at the end of mitosis. J Cell Sci 1999; 112: 2253–64

Boehmer T, Enninga J, Dales S, Blobel G, Zhong H. Depletion of a single nucleoporin, Nup107, prevents the assembly of a subset of nucleoporins into the nuclear pore complex. Proc Natl Acad Sci USA 2003; 100: 981–85

Bonne G, Di Barletta MR,Varnous S, Be´cane HM, Hammouda EH, Merlini L, Muntoni F, Greenberg CR, Gary F, Urtizberea JA, et al. Mutations in the gene encoding lamin A/C cause autosomal dominant Emery-Dreifuss muscular dystrophy. Nat Genet 1999; 21: 285–88.

Boulanger J, Kervrann C, Boulthemy P, Elbau P, Sibarita JB, Salamero J. Patch-based nonlocal functional for denoising fluorescence microscopy image sequences. IEEE Trans Med Imaging 2010; 29: 442-54

Burke B, Ellenberg J. Remodelling the walls of the nucleus. Nat Rev Mol Cell Biol 2002; 3:487-97

Champion L, Linder MI, Kutay U. Cellular reorganization during mitotic entry. Trends Cell Biol 2017; 27: 26-42

Chaudhary, N. & Courvalin, J.-C. Stepwise reassembly of the nuclear envelope at the end of mitosis. J. Cell Biol. 122, 295–306 (1993).

Cronshaw JM, Krutchinsky AN, Zhang W, Chait BT, Matunis MJ. Proteomic analysis of the mammalian nuclear pore complex. J Cell Biol 2002; 158:915-27

D'Angelo MA, Anderson DJ, Richard E, Hetzer MW. Nuclear pores form de novo from the both sides of the nuclear envelope. Science 2006; 312: 440-3

D'Angelo MA, Raices M, Panowski SH, Hetzer MW. Age dependent deterioration of nuclear pore complexes causes a loss of nuclear integrity in post mitotic cells. Cell 2009; 136: 284-95

Daigle N, Beaudouin J, Hartnell L, Imreh G, Hallberg E, Lippincott-Schwartz J, Ellenberg J.. Nuclear pore complexes form immobile networks and have a very low turnover in live mammalian cells. J Cell Biol 2001; 154: 71–84

De Sandre-Giovannoli A, Chaouch M, Kozlov S, Vallat JM, Tazir M, Kassouri N, Szepetowski P, Hammadouche T, Vandenberghe A, Stewart CL, et al. Homozygous defects in LMNA, encoding lamin A/C nuclear-envelope proteins, cause autosomal recessive axonal neuropathy in human (Charcot-Marie-Tooth disorder type 2) and mouse. Am J Hum Genet 2002; 70: 726–36.

Devos D., Dokudovskaya S, Alber F, Williams R, Chait BT, Sali A, Rout MP. Components of coated vesicles and nuclear pore complexes share a common molecular architecture. PLoS Biol 2004; 2, e380

Dultz E, Ellenberg J. Live imaging of single nuclear pores reveals unique assembly kinetics and mechanism in interphase. J Cell Biol 2010; 191:15-22

Dultz E, Zanin E, Wurzenberger C, Braun M, Rabut G, Sitoni L, Ellenberg J. Systematic kinetic analysis of mitotic dis- and reasembly oft he nuclear pore in living cells. J Cell Biol 2008; 180: 857-65

Enarson P, Enarson M, Bastos R, Burke B. Amino-terminal sequences that direct nucleoporin nup153 to the inner surface of the nuclear envelope. Chromosoma 1998; 107: 228–236

Eriksson M, Brown WT, Gordon LB, Glynn MW, Singer J, Scott L, Erdos MR, Robbins CM, Moses TY, Berglund P, et al. Recurrent de novo point mutations in lamin A cause Hutchinson-Gilford progeria syndrome. Nature 2003; 423: 293–8

Fichtman B, Ramos C, Rasala B, Harel A, Forbes DJ. Inner/outer nuclear membrane fusion in nuclear pore assembly. Mol Biol Cell 2010; 21: 4197-211

Ford MG, Mills IG, Peter BJ, Vallis Y, Praefcke GJ, Evans PR, McMahon HT. Curvature of clathrin-coated pits driven by epsin. Nature 2002; 419:361–66

Frosst P, Guan T, Subauste C, Hahn K, Gerace L. Tpr is localized within the nuclear basket of the pore complex and has a role in nuclear protein export. J. Cell Biol. 2002; 156:617–30

Gall JG. Octagonal nuclear pores. J Cell Biol 1967; 32:391–99

Gorjanacz M, Klerkx EP, Galy V, Santarella R, Lopez-Iglesias C, Askjaer P, Mattaj IW. *Caenorhabditis elegans* BAF-1 and its kinase VRK-1 participate directly in post-mitotic nuclear envelop assembly. EMBO J 2007; 26: 132-43

Grossman E, Medalia O, Zwerger M. Functional Architecture of the Nuclear Pore Complex. Annu Rev Biophys 2012; 41: 557-84

Haraguchi T, Kojidani T, Koujin T, Shimi T, Osakada H, Mori C, Yamamoto A, Hiraoka Y. Live cell imaging and electron microscopy reveal dynamic processes of BAF-directed nuclear envelope assembly. J Cell Sci 2008; 121: 2540-54

Haraguchi T, Koujin T, Hayakawa T, Kaneda T, Tsutsumi C, Imamoto N, Akazawa C, Sukegawa J, Yoneda Y, Hiraoka Y. Live fluorescence imaging reveals early recruitment of emerin, LBR, RanBP2, and Nup153 to reforming functional nuclear envelopes. J Cell Sci 2000; 113: 779–94

Haraguchi T, Ding D, Yamamoto A, Kaneda T, Koujin T, Hiraoka Y. Multiple-color fluorescence imaging of chromosomes and microtubules in living cells. Cell Struct Funct 1999; 24, 291-298

Haraguchi T, Koujin, T., Segura-Totten, M., Lee, K.K., Matsuoka, Y., Yoneda, Y., Wilson, K.L., & Hiraoka, Y. BAF is required for emerin assembly into the reforming nuclear envelope. J Cell Sci 2001; 114: 4575-85.

Haraguchi T, Osakada H, Koujin T. Live CLEM imaging to analyze nuclear structures at high resolution. Methods Mol Biol 2015; 1262: 89-103

Harel A, Orjalo A V, Vincent T, Lachish-Zalait A, Vasu S, Shah S, Zimmerman E, Elbaum M, Forbes DJ. Removal of a single pore subcomplex results in vertebrate nuclei devoid of nuclear pores. Mol Cell 2003; 11:853-64

Hase ME, Cordes VC. Direct interaction with nup153 mediates binding of Tpr to the periphery of the nuclear pore complex. Mol Biol Cell 2003; 14:1923–40

Heessen S, Fornerod M. The inner nuclear envelope as a transcription factor resting place. EMBO Rep 2007; 8: 914-19

Hink MA, Griep RA, Borst JW, van Hoek A, Eppink MHM, Schots A, Visser AJWG. Structural dynamics of green fluorescent protein alone and fused with a single chain Fv protein. J Biol Chem 2000; 275: 17556-60

Hoffmann K, Dreger CK, Olins AL, Olins DE, Shultz LD, Lucke B, Karl H, Kaps R, Mu¨ller D, Vaya´ A, et al. Mutations in the gene encoding the lamin B receptor produce an altered nuclear morphology in granulocytes (Pelger-Hue¨t anomaly). Nat Genet 2002; 31: 410–4.

Hu T, Guan T, Gerace L.Molecular and functional characterization of the p62 complex, an assembly of nuclear pore complex glycoproteins. J Cell Biol 1996; 134:589-601

Hurwitz ME, Blobel G. NUP82 is an essential yeast nucleoporin required for poly(A)+ RNA export. J. Cell Biol. 1995; 130:1275–81

Hutten S, Walde S, Spillner C, Hauber J, Kehlenbach RH. The nuclear pore component Nup358 promotes transportin-dependent nuclear import. J. Cell Sci. 2009; 122:1100–10

Iwamoto M, Asakawa H, Ohtsuki C, Osakada H, Koujin T, Hiraoka Y, Haraguchi T. Monoclonal antibodies recognize Gly-Leu-Phe-Gly Repeat of nucleoporin Nup98 of Tetrahymena, Yeasts, and Humans. Monoclon Antib Immunodiagn Immunother 2013; 32: 81-90.

Iwasaki M, Kuwata T, Yamazaki Y, Jenkins NA, Copeland NG, Osato M. Identification of cooperative genes for Nup98-HOXA9 in myeloid leukemogenesis using a mouse model. Blood 2005; 105: 784-93.

Kobayashi S, Kojidani T, Osakada H, Yamamoto A, Yoshimori T, Hiraoka Y, Haraguchi T. Artificial induction of autophagy around polystyrene beads in nonphagocytic cells. Autophagy 2010; 6: 36-45

Kobayashi S, Koujin T, Kojidani T, Osakada H, Mori C, Hiraoka Y, Haraguchi T. BAF is a cytosolic DNA sensor that leads to exogenous DNA avoiding autophagy. PNAS 2015; 112: 7027–32

Kraemer DM, Strambio-de-Castillia C, Blobel G, Rout MP. The essential yeast nucleoporin NUP159 is located on the cytoplasmic side of the nuclear pore complex and serves in karyopherinmediated binding of transport substrate. J. Biol. Chem. 1995; 270:19017–21

Krull S, Thyberg J, Bjorkroth B, Rackwitz HR, Cordes VC. Nucleoporins as components of the nuclear pore complex core structure and tpr as the architectural element of the nuclear basket. Mol Biol Cell 2004; 15: 4261–77

Lin F, Worman HJ. Structural organization of the human gene encoding nuclear lamin A and nuclear lamin C. J Biol Chem 1993; 268: 16321–26

Lim YH, Fahrenkrog B, Köser J, Schwarz-Herion K, Deng J, Aebi U. Nanomechanical Basis of Selective Gating by the Nuclear Pore Complex. Science 2007; 318: 640-43

Lin YW, Slape C, Zhang Z, Aplan PD. Nup98 HOXD13 transgenic mice develop a highly penetrant, severe myelodysplastic syndrome that progress to acute leukemia. Blood 2005; 106:287-95

Lu L. Ladinsky MS, Kirchhausen T. Formation of the postmitotic nuclear envelope from extended ER cisternae precedes nuclear pore assembly. J. Cell Biol 2011; 194: 425-40

Lu X, Shi Y, Lu Q, Ma Y, Lio J, Wang Q, Ji J, Jiang Q, Zhang C. Recruitment for lamin B receptor and its regulation by importin beta and phosphorylation in nuclear envelope assembly during mitotic exit. J Biol Chem 2010; 285: 33281-93

Macaulay C, Forbes DJ. Assembly of the nuclear pore: biochemically distinct steps revealed with NEM, GTP gamma S, and BAPTA. J Cell Biol 1996; 132: 5-20

Mahajan R, Delphin C, Guan T, Gerace L, Melchior F. A small ubiquitin-related polypeptide involved in targeting RanGAP1 to nuclear pore complex protein RanBP2. Cell 1997; 88:97–107

Mattaut A, Dechat T, Adam SA, Goldman RD, Gruenbaum Y. Nuclear lamins, disease and aging. Curr Opin Cell Biol 2006; 18:335-41

Me´sza´ros N, Cibulka J, Mendiburo MJ, Romanauska A, Schneider M, Ko¨hler A. Nuclear Pore Basket Proteins Are Tethered to the Nuclear Envelope and Can Regulate Membrane Curvature. Developmental Cell 2015; 33: 285–98

Mitchell JM, Mansfeld J, Capitanio J, Kutay U, Wozniak RW. Pom121 links two essential subcomplexes of the nuclear pore complex core to the membrane. J Cell Biol 2010; 191:505-21

Nakata T, Terada S, Hirokawa N. Visualization of dynamics of synaptic vesicle and plasma membrane proteins in living axons. J Cell Biol 1998, 140: 659-74

Naylor RM, Jeganathan KB, Cao X, van Deursen JM. Nuclear pore protein Nup88 activates anaphase promoting complex to promote aneuploidy. J.Clin.Investig. 2016; 126: 543-59

Neumann N, Lundin D, Poole AM. Comparative genomic evidence for a complete nuclear pore complex in the last eukaryotic common ancestor. PLoS ONE 2010; 5: e13241

Okita K, Kiyonari H, Mobuhisa I, Kimura N, Aizawa S, Taha T. Targetted disruption of the mouse ELYS gene results in embryonic death atperi-implantation development. Genes Cells 2004; 9: 1083-91

Otsuka S, Steyer AM, Schorb, M, Hériché JK, Hossain MJ, Sethi S, Kueblbeck M, Schwab Y, Beck M, Ellenberg J. Postmitotic nuclear pore assembly proceeds by radial dilation of small membrane openings. Nat Struct Mol Biol 2018; 25: 21-28

Otsuka, S., Bui, K.H., Schorb, M., Hossain, M.J., Politi, A.Z., Koch, B., Eltsov, M., Beck, M., & Ellenberg, J. Nuclear pore assembly proceeds by an inside-out extrusion of the nuclear envelope. Elife, 2016; 5: e19071

Puhka M, Vihinen H, Joensuu M, Jokitalo E. Endoplasmic reticulum remains continuous and undergoes sheet-to-tubule transformation during cell division in mammalian cells. J Cell Biol 2007; 179: 895–909

Puhka, M., Joensuu, M., Vihinen, H., Belevich, I. & Jokitalo, E. Progressive sheet-to-tubule transformation is a general mechanism for endoplasmic reticulum partitioning in dividing mammalian cells. Mol. Biol. Cell. 2012; 23: 2424-32.

Quijano-Roy S, Mbieleu B, Bonnemann CG, Jeannet PY, Colomer J, Clarke NF, Cuisset JM, Roper H, De Meirleir L, D'Amico A, et al. De novo LMNA mutations cause a new form of congenital muscular dystrophy. Ann Neurol 2008; 64: 177–86

Rasala BA, Orjalo AV, Shen Z, Briggs S, Forbes DJ. ELYS is a dual nucleoporin/kinetochore protein required for nuclear pore assembly and proper cell division, Proc. Natl. Acad. Sci. U. S. A. 2006; 103: 17801–806

Reichelt R, Holzenburg A, Buhle EL, Jarnik M, Engel A, Aebi U. Correlation between structure and mass distribution of the nuclear pore complex and of distinct pore complex components. J Cell Biol 1990; 110(4):883-94

Reddy KL, Zullo JM, Bertolino E, Singh H. Transcriptioonal repression mediated by repositioning of genes to nuclear lamina. Nature 2008; 452: 243-47

Sakuma S, D'angelo A. The role of the nuclear pore complex in cellular dysfunction aging and disease. Sem in Cell and Dev Biol 2017; 68:72-84

Schellhaus AK, De Magistris P, Antonin W. Nuclear reformation at the end of mitosis. J Mol Biol 2015; 128: 3466-77

Schirmer EC, Gerace L. The nuclear membrane proteome: extending the envelope. Trends Biochem Sci 2005; 30: 551-58

Schindelin J, Arganda-Carreras I, Frise E, Kaynig V, Longaur M, Poetzsch T, Preibisch S, Rueden C, Saalfeld S, Schmid B, Tinevez JY, White DJ, Hartenstein V, Eliceiri K, Tomancak P, Cardona A. Fiji: an open-source platform for biological-image analysis. Nat Methods 2012; 9: 676-82

Schwartz M, Travesa A, Martell SW, Forbes DJ. Analysis of the initiation of nuclear pore assembly by ectopically targeting nucleoporins to chromatin. Nucleus 2015; 6: 40-54

Schwartz TU, Modularity within the architecture of the nuclear pore complex. Curr Opin Struct Biol 2005; 15:221–26

Segura-Totten M, Kowalski AK, Craigie R, Wilson KL. Barrie-to-autointegration factor: major roles on chromatin decondensation and nuclear assembly. J Cell Biol 2002; 158: 475-85

Sheehan MA, Mills AD, Sleeman AM, Laskey RA, Blow JJ. Steps in the assembly of replication-competent nuclei in a cell-free system from Xenopus egg. J Cell Biol 1988; 106: 1-12

Siniossoglou S, LutzmannM, Santos-Rosa H, Leonard K,Mueller S, et al. Structure and assembly of the Nup84p complex. J. Cell Biol. 2000; 149:41–54

Smitherman M, Lee K, Swanger J, Kapur R, Clurman BE. Characterization and targeted disruption of murine Nup50 a p27(Kip1) interacting component of the nuclear pore complex. Mol. Cell Biol. 2000; 20: 5631-42

Vasu S, Shah S, Orjalo A, Park M, Fischer WH, Forbes DJ. Novel vertebrate nucleoporins Nup133 and Nup160 play a role in mRNA export. J Cell Biol 2001; 155: 339–54

Vietri M, Schink KO, Campsteijn C, Wegner CS, Schultz SW, Christ L, Thoresen SB, Brech A, Raiborg C, Stenmark H. Spastin and ESCRT-III coordinate mitotic spindle disassembly and nuclear envelope sealing. Nature 2015; 522: 231–35

Vollmer B, Antonin W. The diverse roles of the Nup93/Nic96 complex proteins – structural scaffolds of the nuclear pore complex with additional cellular functions. Biol Chem 2014; 395:515-28

Vollmer B, Lorenz M, Moreno-Andre´s D, Bodenho¨ fer M, De Magistris P, Astrinidis SA, Schooley A, Flo¨ tenmeyer M, Leptihn S, Antonin W. Nup153 Recruits the Nup107-160 Complex to the Inner Nuclear Membrane for Interphasic Nuclear Pore Complex Assembly. Developmental Cell 2015; 33, 717-728

Walther TC, Alves A, Pickersgill H, Loiodice I, Hetzer M, Galy V, Hulsmann BB, Kocher T, Wilm M, Allen T, Mattaj IW, Doye V. The conserved Nup107-160 complex is critical for nuclear pore complex assembly. Cell 2003a; 113:195–206

Walther TC, Askjaer P, Gentzel M, Habermann, Griffiths G, Wilm M, Mattaj IW, Hetzer M. RanGTP mediates nuclear pore complex assembly. Nature 2003; 424: 689-94

Worman HJ, Courvalin JC. The inner nuclear membrane. J Membr Biol 2000; 117: 1-11

Wu X, Kasper LH, Mantcheva RT, Mantchev GT, Springett MJ, van Deursen JM. Disruption of the FG nucleoporin NUP98 causes selective changes in nuclear pore complex stoi-chiometry and function. Proc Natl Acad Sci U S A 2001; 98: 3191– 96

Xu XM, Rose A, Muthuswamy S, Jeong SY, Venkatakrishnan S, Zhao Q, Meier I. NUCLEAR PORE ANCHOR, the Arabidopsis homolog of Tpr/Mlp1/Mlp2/megator, is involved in mRNA

export and SUMO homeostasis and affects diverse aspects of plant development. Plant Cell 2007; 19:1537–48

Yang L, Guan T, Gerace L. Integral membrane proteins of the nuclear envelope are dispersed throughout the endoplasmic retic- ulum during mitosis. J Cell Biol 1997; 137:1199–210

Ye Q, Callebaut I, Pezhman A, Courvalin JC, Worman HJ. Domain-specific interactions of human HP1-type chromodomain proteins and inner nuclear membrane protein LBR. J Biol Chem 1997; 272: 14983-89.

Zhang X, Chen S, Yoo S, Chakrabarti S, Zhang T, Ke T. Mutation in nuclear pore component Nup155 leads to atrial fibrillation and early sudden cardiac death. Cell 2008; 135: 1017-27

Zierhut C, Jennsess C, Kimura H, Funabiki H. Nucleosomal regulation of chromatin composition and nuclear assembly revealed by histone depletion. Nat Struct Mol Biol 2014; 21: 617-25

Achievements

Sukriye Bilir, Tomoko Kojidani, Yasushi Hiraoka, Tokuko Haraguchi..Live CLEM imaging reveals the nuclear envelope precursor membrane to post-mitotically assemble the nuclear pore complex. BMB2015-Biochemistry and Molecular Biology meeting, 1-4 December 2015, Kobe port island

Sukriye Bilir, Tomoko Kojidani, Yasushi Hiraoka, Tokuko Haraguchi. A novel model for nuclear pore complex formation at the end of mitosis. The 68th Annual Meeting of the Japan Society for Cell Biology, 15-17 June 2016, Kyoto Terrsa

Sukriye Bilir, Tomoko Kojidani, Yasushi Hiraoka, Tokuko Haraguchi. The structure of ER plays an important role for the NPC reformation at the end of mitosis. MBSJ2016-The 39th Annual Meeting of the Molecular Biology Society of Japan, 30 November-2 December 2016, Pacifico Yokohama

Sukriye Bilir, Shouhei Kobayashi,Takako Koujin, Chie Mori, Hiroko Osakada, Tomoko Kojidani, Yasushi Hiraoka, Tokuko Haraguchi. NPC formation on the nucleoporin-beads incorporated into living cells. The 69th Annual Meeting of the Japan Society for Cell Biology, 13-15 June 2017, Sendai International Center

Yuka Suzuki,Sukriye Bilir,Hiroko Osakada, Shouhei Kobayashi, Yasushi Hiraoka, Tokuko Haraguchi, Kazuo Yamagata. Understanding of nuclear assembly in mouse preimplantation embryo by reconstitution approach. 1st HMGU- Japan Epigenetics and Chromatin Symposium, 4-6 September 2017, Helmholtz Zentrum München

Sukriye Bilir, Shouhei Kobayashi,Takako Koujin, Chie Mori, Hiroko Osakada, Tomoko Kojidani, Yasushi Hiraoka, Tokuko Haraguchi. NPC formation on the nucleoporin-beads

incorporated into living cells. ConBio2017-The 40th Annual Meeting of Molecular Biology Society of Japan, 6-9 December 2017, Kobe Port Island

Tokuko Haraguchi, Shouhei Kobayashi, Sukriye Bilir, Takako Koujin, Hiroko Osakada, Tomoko Kojidani, Chie Mori, Sahashi Ritsuko, Yasushi Hiraoka. Bead-induced assembly of the artificial nucleus in the living cell. ConBio2017-The 40th Annual Meeting of Molecular Biology Society of Japan, 6-9 December 2017, Kobe Port Island

Kazuo Yamagata, Yuka Suzuki, Sukriye Bilir, Hiroko Osakada, Shouhei Kobayashi, Yasushi Hiraoka, Tokuko Haraguchi. Nuclear assembly mechanism in mammalian fertilized oocyte revealed by quantitative and reconstitution approach. ConBio2017-The 40th Annual Meeting of Molecular Biology Society of Japan, 6-9 December 2017, Kobe Port Island

Yuka Suzuki, Sukriye Bilir, Hiroko Osakada, Shouhei Kobayashi, Yasushi Hiraoka, Tokuko Haraguchi, Kazuo Yamagata. Understanding of nuclear assembly in mouse preimplantation embryo by reconstitution approach. ConBio2017-The 40th Annual Meeting of Molecular Biology Society of Japan, 6-9 December 2017, Kobe Port Island

Sukriye Bilir, Shouhei Kobayashi, Takako Koujin, Chie Mori, Hiroko Osakada, Tomoko Kojidani, Yasushi Hiraoka, Tokuko Haraguchi. A role of Nup133 and Nup153 on the post-mitotic nuclear pore complex formation. MBSJ2018-The 41st Annual Meeting of the Molecular Biology Society of Japan, 28-30 November 2018, Pacifico Yokohama

Yuka Suzuki, Sukriye Bilir, Hiroko Osakada, Shouhei Kobayashi, Yasushi Hiraoka, Tokuko Haraguchi, Kazuo Yamagata. Reconstruction of nuclei in mouse preimplantation embryo by DNA-beads. MBSJ2018-The 41st annual meeting of the Molecular Biology Society of Japan, 28-30 November 2018, Pacifico Yokohama

Sukriye Bilir, Tomoko Kojidani, Chie Mori, Shouhei Kobayashi, Takako Koujin, Yasushi Hiraoka and Tokuko Haraguchi. Roles of Nup133, Nup153, and membrane fenestrations in

assembly of the nuclear pore complex at the end of mitosis. Genes to Cells, in press, accepted on 1 March 2019.

Yuka Suzuki, Sukriye Bilir, Hiroko Osakada, Shouhei Kobayashi, Yu Hatano, Daisuke Mashiko, Yasushi Hiraoka, Tokuko Haraguchi, Kazuo Yamagata. Nuclear reconstitution in mouse fertilized egg originated from DNA-coated beads. Scientific Reports, in revision, submitted on 21 January 2019.

Acknowledgements

Firstly, I would like to express my deep appreciation and thanks to my supervisors and mentors Prof. HARAGUCHI Tokuko and Prof. HIRAOKA Yasushi for being supportive, helpful and genial during my Ph.D. study and related research. Their guidance helped me all the time during my Ph.D. research and writing this thesis.

Besides my supervisors, I would like to thank to the preliminary defense committee: Prof. KAI Toshie, Prof. NAMBA Keiichi and Prof. FUKAGAWA Tatsuo for their mind opening questions.

I thank to my fellow lab mates for all the help, patience and for all the fun we had in the last 5 years.

Lastly, I would like to thank my family for not hesitating to give any help to me in my entire life.